CORA Cork Open Research Archive
Cartlann Taighde Oscailte Chorcaí

Title	Synthesis of 1,2,5-oxathiazole-S-oxides by 1,3 dipolar cycloadditions of nitrile oxides to α-oxo sulfines
Authors	McCaw, Patrick G.;Khandavilli, Udaya Bhaskara Rao;Lawrence, Simon E.;Maguire, Anita R.;Collins, Stuart G.
Publication date	2018-12-12
Original Citation	McCaw, P. G., Khandavilli, U. B. R., Lawrence, S. E., Maguire, A. R. and Collins, S. G. (2018) 'Synthesis of 1,2,5-oxathiazole-S-oxides by 1,3 dipolar cycloadditions of nitrile oxides to α-oxo sulfines', Organic and Biomolecular Chemistry, 17(3), pp. 622-638. doi:10.1039/C8OB02691B
Type of publication	Article (peer-reviewed)
Link to publisher's version	10.1039/C8OB02691B
Rights	© 2018, the Authors. Published by the Royal Society of Chemistry. All rights reserved.
Download date	2026-11-16 05:02:02
Item downloaded from	https://hdl.handle.net/10468/7494

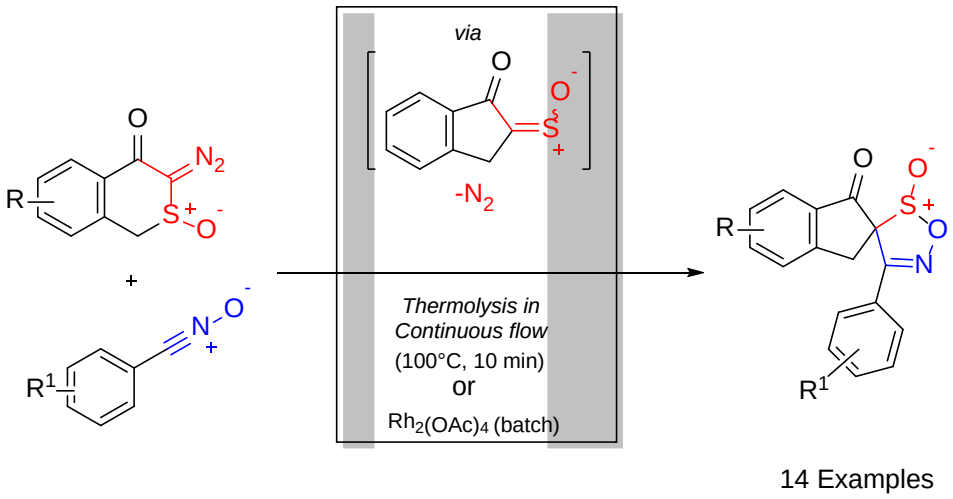
UCC
University College Cork, Ireland
Coláiste na hOllscoile Corcaigh

Synthesis of 1,2,5-oxathiazole-S-oxides by 1,3 dipolar cycloadditions of nitrile oxides to α-oxo sulfines

Patrick G. McCaw,[a] U. B. Rao Khandavilli ,[a] Simon E. Lawrence,[a] Anita R. Maguire,*[b] Stuart G. Collins.*[a]

[a] *School of Chemistry, Analytical and Biological Chemistry Research Facility, Synthesis and Solid State Pharmaceutical Centre, University College Cork, Ireland. E-mail: stuart.collins@ucc.ie*

[b] *School of Chemistry and School of Pharmacy, Analytical and Biological Chemistry Research Facility, Synthesis and Solid State Pharmaceutical Centre, University College Cork, Ireland. Fax: +353(0)214274097; Tel: +353(0)214901694; E-mail: a.maguire@ucc.ie*



Abstract

Synthetic methodology for the generation of novel 1,2,5-oxathiazole-*S*-oxides from cycloaddition of nitrile oxide dipoles with α-oxo sulfines generated in situ via the α-sulfinyl carbenes derived from α-diazosulfoxides is described. Experimental evidence and mechanistic rationale for the unanticipated interconversion of the diastereomeric 1,2,5-oxathiazole-*S*-oxide cycloadducts are discussed. Notably, using rhodium acetate as a catalyst at 0°C under traditional batch conditions led to the selective formation and isolation of the kinetic isomers, while, in contrast, using continuous flow thermolysis, optimal conditions for the synthesis and isolation of the thermodynamic isomers were established.

Introduction

Heterocyclic systems are common motifs in biologically active compounds including pharmaceuticals and natural products. [1-4] While 1,4,2-oxthiazoles are commonly reported and described in the literature,[5,6] the regioisomeric 1,2,5-oxathiazole has only rarely been described.[7,8] In 1,3-dipolar cycloaddition reactions between nitrile oxide and thioketones, the 1,4,2-oxathiazole is formed regioselectively in preference to the 1,2,5-oxathiazole.[9] 1,4,2-Oxathiazoles can be envisaged as sulfur analogues of 1,2,4-oxadiazoles which have been found to show anticancer activity *via* inducing apoptosis.[9] In addition to the widely reported 1,4,2-oxathiazoles, there are a few reported examples of 1,4,2-oxathiazole-*S*-oxides.[10]

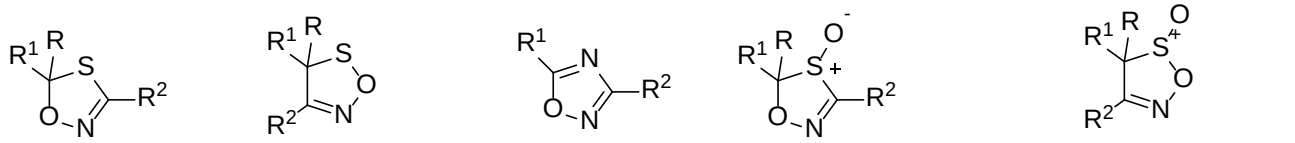
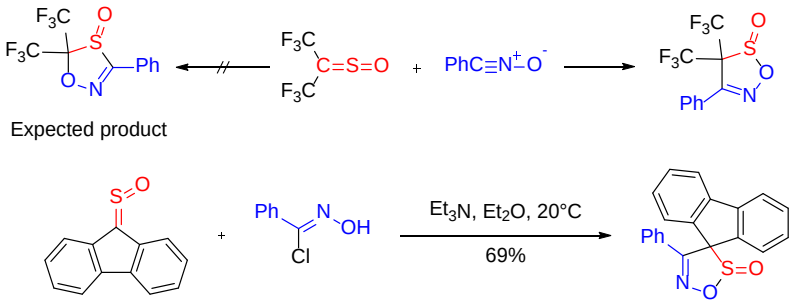


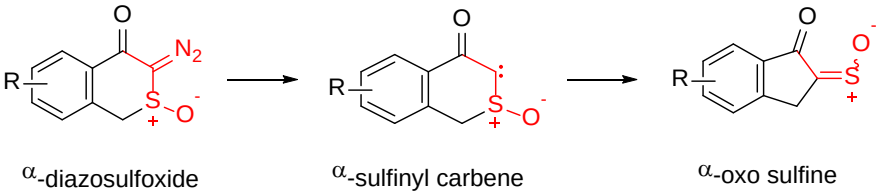
Figure 1 Five membered heterocyclic motifs

To the best of our knowledge, there are no reported examples of a general synthetic method to access 1,2,5-oxathiazoles or the corresponding 1,2,5-oxathiazole-*S*-oxides. There are only two example of 1,2,5-oxathiazole-*S*-oxide in the literature, and in both cases the heterocycle is described as an unexpected product formed from cycloaddition of sulfines (Scheme 1), while the opposite regiochemistry is normally preferred.[10-12] Interestingly, of the two reported 1,2,5-oxathiazole-*S*-oxides in the literature, Zwanenburg has investigated the thermal fragmentation of one 1,2,5-oxathiazole-*S*-oxide which was isolated as an unexpected regioisomer from the cycloaddition of fluorinethione-S-oxide and benzonitrile oxide.[10,11] The thermal fragmentation of 1,4,2-oxathiazoles has been used as a method to access isothiocyanates with the rearrangement occurring under mild thermal conditions.[13,14] Highlighting the interest in these types of compounds, is a recent report by Pierce which focused on the synthesis of 1,4,2-oxathiazoles, through oxidative cyclisation of thiohydroximic acids,[5] as well as a report by Mloston who generated fluorinated 1,4,2-oxathiazoles through regioselective cycloaddition reactions of fluorinated nitrile oxide with thioketones.[6]



Scheme 1: Synthesis of 1,2,5-oxathiazole-S-oxides.

Previously our research group has reported the transformation of α-diazosulfoxides to α-oxo sulfines *via* a hetero-Wolff rearrangement of the intermediate α-sulfinyl carbene (Scheme 2). This transformation occurs under a range of mild reaction conditions including transition metal catalysis, thermolysis, microwave irradiation and photolysis.[15-17] Trapping as Diels-Alder cycloadducts has confirmed the intermediacy of α-oxo sulfines.[16,18] While in early work, modest yields of α-diazosulfoxides were achieved, we have recently demonstrated that they are more readily accessible through use of continuous flow in high yields under mild conditions. Accordingly their use as synthetic precursors to highly functionalised heterocyclic scaffolds is now feasible.[17-21] Recently, the advantages[22-27] of flow chemistry such as an enhanced safety profile,[20,22] faster scale up,[28,29] library synthesis,[30] green chemistry,[31,32] online analysis[33] and self-optimising reactors[34,35] have all been described. These advantages have been utilised across a range of reaction types including high temperature reactions,[36] organometallic reactions,[37,38] and photochemical transformations.[39-41]



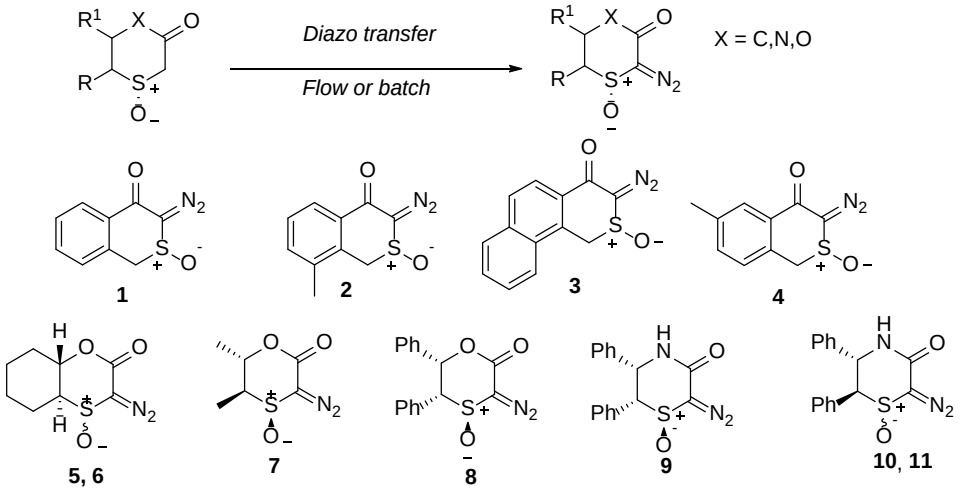
Scheme 2: Rearrangement of α-diazosulfoxide to α-sulfine via *hetero-Wolff rearrangement.*

While cycloaddition to sulfines and α-oxo sulfines is well established, in many instances the cycloadducts are labile and undergo subsequent rearrangement to more stable species.[10,42-44] While examples of dipolar cycloadditions have been described in continuous flow,[45-47] herein we describe dipolar cycloaddition of α-oxo sulfines derived from α-diazosulfoxides[48] under mild reaction conditions with nitrile oxides to form oxathiazole-*S*-oxides is described. Most interestingly, the stereochemical outcome of the transformations can be directed by alteration of the reaction conditions.

Results and Discussion

While the original synthesis of α-diazosulfoxides was reported 20 years ago, their synthetic utility was limited by poor yields and difficulty in accessing synthetically useful quantities of these liable compounds. Recently we have demonstrated that improved yields and efficiencies can be obtained through use of continuous flow reaction conditions for the diazo transfer step, which overcame the sensitivity of the products to basic reaction conditions by removing the product from the immobilised base as it formed (Scheme 3).[19,48]

For this study of dipolar cycloadditions with nitrile oxides, sulfines generated from the ketone derived alpha-diazosulfoxides **1-4** were selected for investigation.

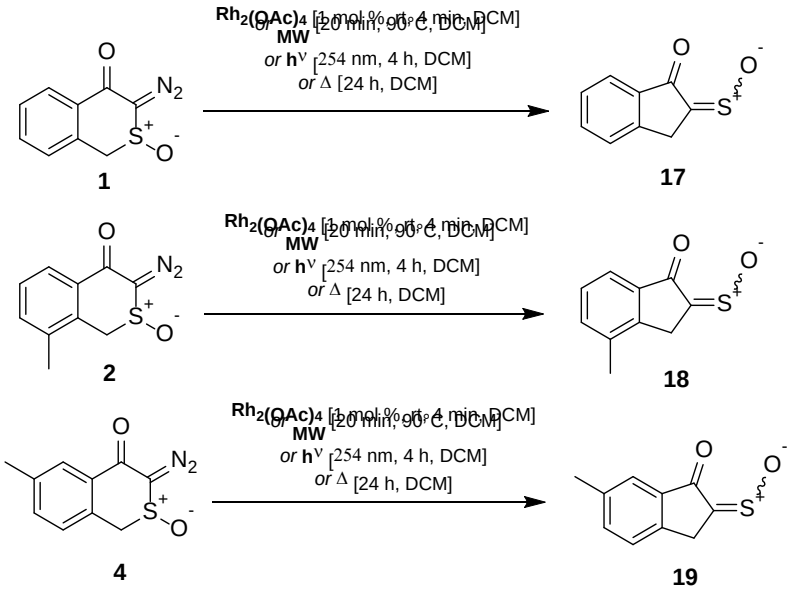


Scheme 3: Range of α-diazosulfoxides synthesised in flow or batch

While nitrile oxide dipoles are usually generated *in situ* by base mediated dehydrohalogenation of the imidoyl chloride, these conditions would not be compatible with base labile α-diazosulfoxides[19] and their transformation to α-oxo sulfines. Nitrile oxides **12–16** were selected for investigation to enable exploration of electronic effects and steric effects of substituted aryl rings. While a few isolated examples of the generation of nitrile oxide dipoles in the absence of base have been recently described, in this event our previously reported strategy for pre-generation of the dipole proved successful.[49]

Cycloadditions of nitrile oxide dipoles with ketone derived α-oxo sulfines.

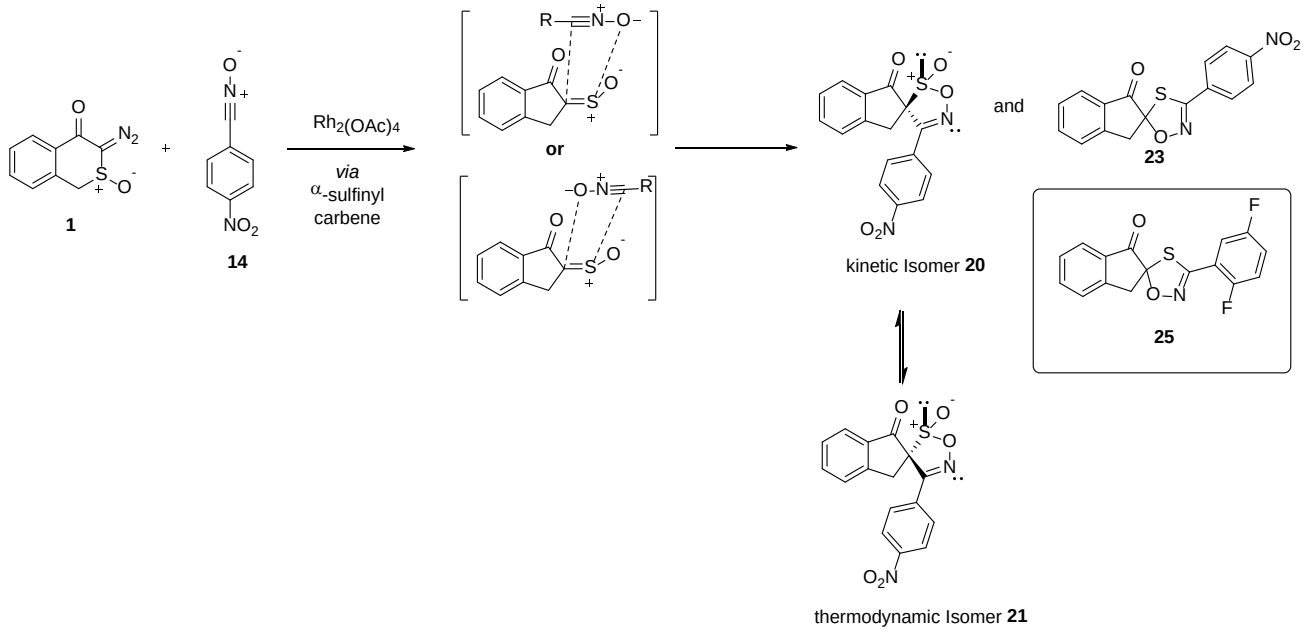
The α-diazosulfoxides **1, 2**, and **4** were synthesised according to the work described earlier and, for each of these carbene precursors, the hetero-Wolff rearrangement was initiated under a range of different conditions, resulting in the corresponding α-oxo sulfines **17**, **18**, and **19** (Scheme 4).[19,18,48] Initial investigations focused on the hetero-Wolff rearrangement of the α-diazosulfoxide **1** to form the α-oxo sulfine **17** *via* the α-sulfinyl carbene intermediate, and subsequent treatment with a nitrile oxide to establish the feasibility of dipolar cycloaddition.



Scheme 4

Reaction of the α-oxo sulfine **17**, generated from α-diazosulfoxide **1** under rhodium acetate catalysis, with *p*-nitrobenzonitrile oxide **14** as an *in situ* trap, in batch reaction conditions was undertaken using the freshly re-generated nitrile oxide dipole to avoid unnecessary exposure of the α-diazosulfoxide **1** to basic conditions. Following stirring for 1h ^{1}H NMR spectroscopy indicated complete consumption of both the α-diazosulfoxide **1** and intermediate α-oxo sulfine **17**. On concentration, ^{1}H NMR spectroscopy of the crude product indicated a mixture of regioisomers (1,2,5-oxathiazole-*S*-oxides and 1,4,2-oxathiazole-*S*-oxides) and diastereomers. These components were later identified (see below) as the kinetic 1,2,5-oxathiazole-*S*-oxide **20**, the thermodynamic 1,2,5-oxathiazole-*S*-oxide **21**, a 1,4,2-oxathiazole-*S*-oxide regioisomer **22** and a 1,4,2-oxathiazole reduction product **23**, in the ratio of 40 : 29 : 22 : 9. No evidence was observed for a second diastereomer of the 1,4,2-oxathiazole-S-oxide regioisomer **24**.

Chromatographic purification of the crude reaction mixture led to the isolation of two pure cycloadducts: the kinetic diastereomer **20** and the 1,4,2-oxathiazole **23**, both of which had been observed in the ^{1}H NMR spectrum of the crude product mixture, while the thermodynamic isomer **21** was not isolated as a pure compound. The structure of the reduction product **23** was assigned by comparison to spectroscopic data reported for similar 1,4,2-oxathiazoles[5,9] and was confirmed by a crystal structure of an analogous compound in the series, **25**, obtained during this work.



Scheme 5: Initial investigation in to the cycloaddition reaction

Determination of the regio- and stereochemistry of the cycloadducts proved interesting. When a pure sample (by ^{1}H NMR) of the major cycloadduct **20** was recrystallised from dichloromethane/toluene, X-ray crystallography revealed the structure as the 1,2,5-oxathiazole-*S*-oxide illustrated in Figure 2. Following crystal structure determination, the single crystal used was recovered from the crystallographic pin and re-analysed by ^{1}H NMR spectroscopy (600 MHz) to unambiguously confirm the relative stereochemistry. Unexpectedly it was clear that the compound present was no longer **20**, but had rearranged to compound **21** isolated following recrystallisation. Following this unanticipated observation, the conversion of the initially isolated kinetic diastereomer to the more stable thermodynamic diastereomer was subsequently seen and monitored across the series of regioisomeric compounds (vide infra).

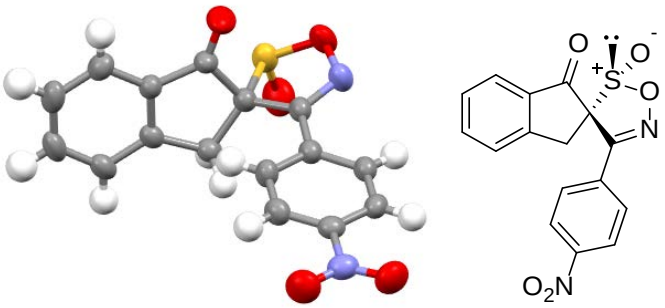
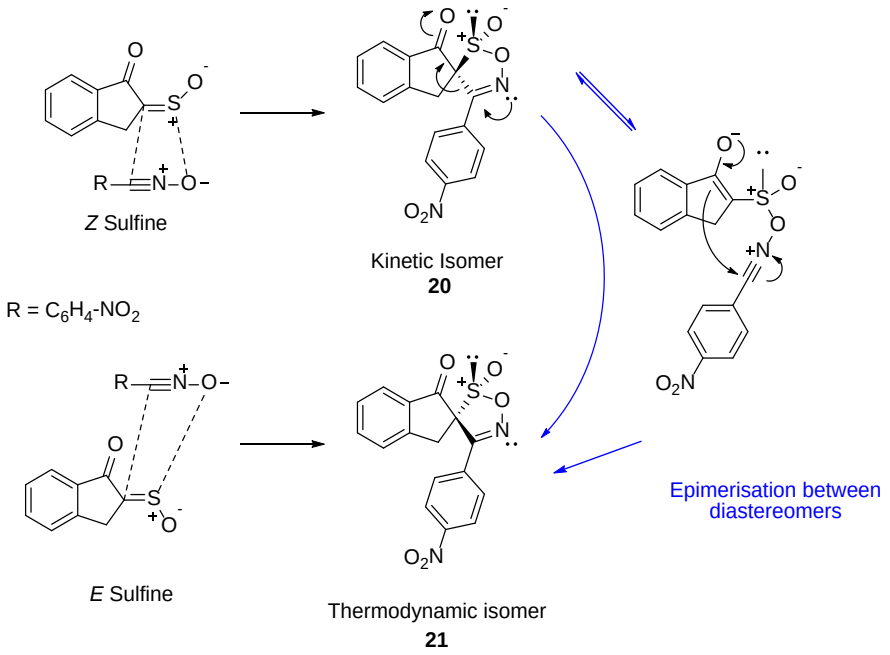


Figure 2: Relative stereochemistry of the 1,2,5-oxathiazole-S-oxide **21**.

This interesting observation suggested interconversion between a kinetic isomer **20** which was originally isolated and the thermodynamic isomer **21**. Analysis of the remaining solid sample that the crystal was taken from, showed approximately a 1:1 ratio of the diastereomers **20** and **21**. Thus it appears, the kinetic cycloadduct **20**, formed by cycloaddition of the nitrile oxide dipole, to the kinetically favoured *Z*-sulfine, interconverts to the isomer **21** over time. Subsequent direct observation of this interconversion by ^{1}H NMR spectroscopy is included in the ESI. Previously, low yields of cycloadducts from dipolar additions of sulfines had been rationalised by the ability to easily undergo cycloreversion reaction.[22,50-54] However, transformation of a kinetic diastereomer to a more stable thermodynamic

diastereomer was an unexpected property of these heterocyclic compounds. Zwanenburg *et al.*[52] have described 1,3-dipolar cycloaddition of sulfines with diphenylnitrilimine to lead to a 1:1 mixture of 1,3,4-thiadiazoline-*S*-oxides which lose their stereochemical integrity over time due to interconversion through a ring opened intermediate.[52]

While formation of the major kinetic diastereomer **20** is envisaged from cycloaddition of the nitrile oxide to the *Z* sulfine as illustrated in Scheme 6, notably, the formation of the cycloadduct **21** can be envisaged by two pathways: either by interconversion of the kinetic isomer **20**, as directly evidenced by crystallographic and spectroscopic studies, or potentially through cycloaddition to the *E* α-oxo sulfine, which cannot be ruled out as a competing cycloaddition pathway. The interconversion of the kinetic cycloadduct **20** to the thermodynamic isomer **21** can be rationalised via a zwittterionic intermediate as illustrated in Scheme 6. From the crystal structure of the thermodynamic isomer **21** (Figure 2), it is clear that the two electron rich oxygen atoms are pointing away from each other. In the kinetic isomer **20**, due to the opposite stereochemistry at the spiro centre, repulsion between the two oxygen atoms would be anticipated, providing a driving force for the rearrangement from the kinetic isomer **20**, to the thermodynamic isomer **21.**



Scheme 6

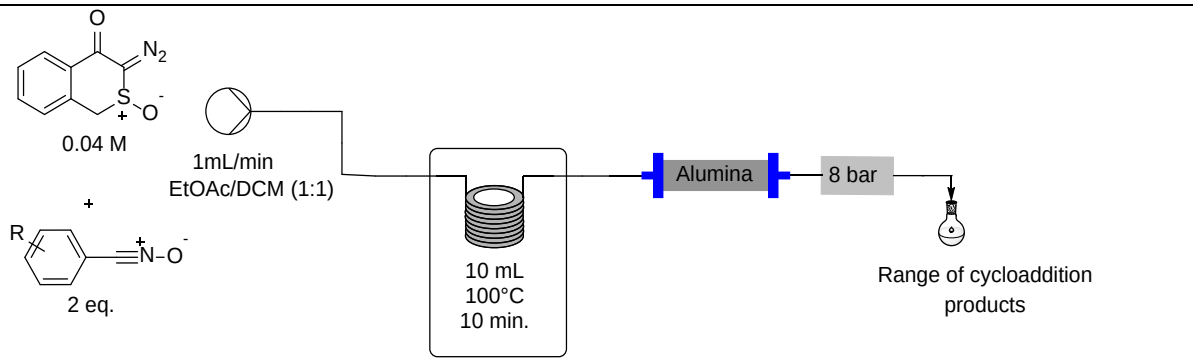
Alternatively the interconversion of the kinetic isomer **20** and the thermodynamic isomer **21** can be rationalised via a cycloreversion reaction to re-form the α-oxo sulfine and nitrile oxide, which subsequently undergo a cycloaddition to form the thermodynamically favoured isomer **21**. There is no experimental evidence to support this pathway.

To confirm that this rearrangement occurred consistently across the series of compounds, the interconversion from the kinetic isomer to the thermodynamic isomer was monitored over time by ^{1}H NMR spectroscopy, for a number of cycloadducts (**20** to **21**, **32** to **31, 35** to **34**), and the data are presented in the ESI.

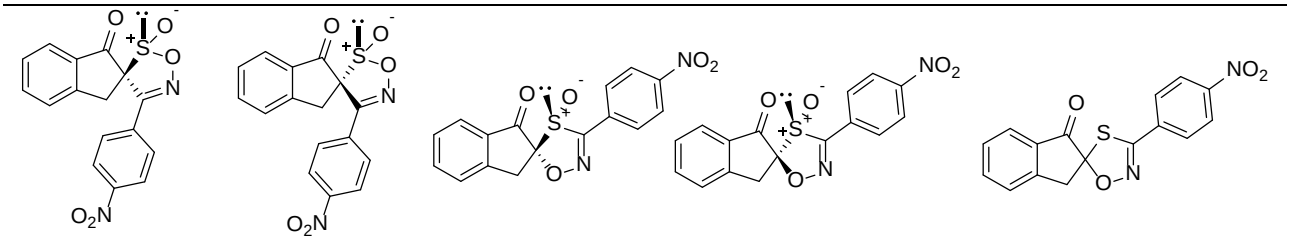
Optimisation of reaction conditions to form cycloadducts

A series of reaction conditions were investigated to establish the optimum conditions for the preferential formation of the thermodynamic isomer of the 1,2,5-oxathiazole-*S*-oxide products which proved to involve thermolysis (10 minutes) in continuous flow (Table 1, entry 7). The investigation began with batch conditions, inducing the hetero-Wolff rearrangement using transition metal catalysis (Table 1, entries 1-3), or thermolysis. Use of microwave irradiation also successfully promoted the cycloaddition reaction with desired product isolated in 18 % yield following chromatography. With long reaction times required in batch for preferential generation of the thermodynamic isomer, and the limitations on scale in microwave reactions, continuous flow conditions were next investigated (Table 1). α-Oxo sulfine generation via transition metal catalysis or thermolysis were explored in continuous flow, with a much cleaner transformation occurring in the absence of the catalyst rhodium acetate. Thermolysis reactions in continuous flow have recently been used for the generation of various reactive intermediates including ketenes and nitrenes.[55-57] Based on a report in the literature that a neutral alumina bed can be used for the removal of excess nitrile oxide and furoxan dimers, in a continuous flow process, this was utilised in this work (Table 1, entry 7).[58] Furthermore, inclusion of an alumina column in line prevents further reactions occurring in the collection flask by removal of unreacted dipole from the reaction outflow. The crude material from this entry was then recrystallized from ether and hexane to give the pure cycloadduct **21** in 52% yield.

*Table 1: Investigation of the impact of reaction conditions on the 1,3-dipolar cycloaddition**



(Conditions used in entry 7)



Kinetic Diastereomer **(K)** | Thermodynamic Diastereomer **(T)** | Regioisomer A **(A)** | Regioisomer B **(B)** | 1,4,2-Oxathiazole **(C)**

	20	**21**	**24**	**22**	**23**
Entry	**Method** (Solvent)	**Generation of α-oxo sulfine**	**Reaction Time** (min)	**Dipole Eq.**	**Ratio[g]** K : T : A : B : C 20 : 21 : 24 : 22 : 23 *(yield)*

1	Batch at r.t. (EtOAc/DCM, 1:1)	$Rh_2(OAc)_4$ (5 mol %)	60	2.3	40 : 29 : 0 : 22 : 9 24% : 0 : 0 : 0 : 15%
2	Batch (CH_3CN/DCM, 1:1)	$Rh_2(OAc)_4$ (5 mol %)	30 (r.t.) 390 (100°C)	4	1 : 1.2 : 0 : 0 : 0 : 5.3(26) 1 : 3.3 : 0 : 0 : 0 : 11.3(26)[f] 0 : 25% : 0 : 0 : 0 : 42%[f]
3	Batch at r.t. (EtOAc/DCM, 1:1)	$Rh_2(OAc)_4$ (5 mol %)	90	4	4 : 3 : 0 : trace : *0* *0 : 17% : 0 : 0 : 0*
4	Microwave (100°C) (DCM)	MW	10	2.5	9 : 81 : 0 : 9 : 0 0 : 18% : 0 : 0 : 0
5	Flow[b] (100°C) (DCM)	Thermolysis[a]	10	4	25 : 50 : 0 : 0 : 0[f]
6	Batch (-20°C)[d] (Et_2O)	$Rh_2(OAc)_4$ (5 mol %)	180	1	*Complex Mixture*[e]
7	Flow[b,c] (100°C) (EtOAc/DCM, 1:1)	Thermolysis[a]	10	2	10 : 56 : 0 : 14 : 0 0 : 52% : 0 : 0 : 0
8	Flow[b,c] (100°C) (EtOAc/DCM, 1:1)	Thermolysis[a]	30	2	*10 : 83 : 0 : 7 : 0*[e]
9	Flow[b,c] (100°C) (EtOAc/DCM, 1:1)	Thermolysis[a]	10	4	*17 : 72 : 0 : 11 :0*[e]
10	Flow[b,c] (r.t.) (EtOAc/DCM, 1:1)	$Rh_2(OAc)_4$ (5 mol %)	60	2	*52 : 38 : 0 : 10 : 0*[e]
11	Batch (r.t.) (EtOAc/DCM, 1:1)	$Rh_2(OAc)_4$ (5 mol %)	30	2	*57 : 43 : 0 : 18 : 0*[e]
12	Batch (0°C) (EtOAc/DCM, 1:1)	$Rh_2(OAc)_4$ (5 mol %)	30	2	*58 : 29 : 0 : 3 : 10*[e]

[a]Thermolysis reactions were carried out at 100°C in continuous flow.
[b]All continuous flow reaction were carried out with an 8 bar back pressure regulator fitted to the system.
[c]A packed bed of alumina was used in a 10 mm id Omnifit® glass column.
[d] Carried out at -20°C.[59]
[e]The crude reaction mixture was not purified
[f] The major product was the oxadiazole from the cycloaddition of the nitrile oxide dipole and the solvent, acetonitrile.
[g] The ratio of product in the crude material was determined by integration of the CH_2 signals alpha to the spiro centre.
* Flow reactions conducted using a Vapourtec E-Series reactor (Vapourtec V3 peristaltic pumps), solution was pumped through a 10 mL reaction coil (Vapourtec part number 50-1011) heated to 100°C at a rate of 1 mL/min giving a residence time of 10 min, followed by a 10 mm id Omnifit™ glass column (Vapourtec part number 30-3296) packed with Alumina (volume ~ 1 mL). PFA tubing was used throughout the system. The reaction mixture passed through a fixed 7 bar back pressure regulator (Kinesis part no. P-787), the crude material was collected as an orange solution and concentrated under reduced pressure.

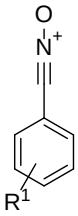
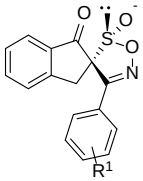
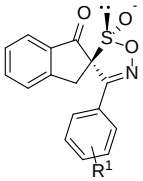
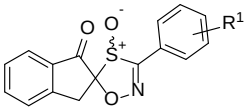
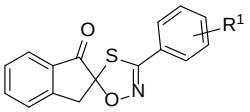
From this investigation of the impact of variation of the reaction conditions, it is clear that carrying out the reaction using the rhodium acetate catalyst, in batch reaction conditions, at 0°C to room temperature favours the selective formation of the kinetic isomer, which can be isolated and fully characterised before interconversion. Thus, reaction conditions were established for the preferential formation of either of the two diastereomeric products which were subsequently applied to a range of substrates.

Isolation of kinetic 1,2,5-oxathiazole-*S*-oxides

With reaction conditions established for the preferential formation and isolation of the kinetic Isomer **20** in pure form, generation and isolation of a series of kinetic 1,2,5-oxathiazole-*S*-oxides using a range of nitrile oxide dipoles, **12–16** was undertaken in order to confirm that the unanticipated conversion to the more stable thermodynamic isomer is consistent across the series. The kinetic isomers were generated in batch reaction conditions, at 0°C with 2 equivalents

of the dipole in each case. Each of the nitrile oxide dipoles **12–16** were pre-generated as a solution in dichloromethane and added to the corresponding α-diazosulfoxide. This was followed directly by addition of rhodium acetate dimer to promote the hetero-Wolff rearrangement of the α-sulfinyl carbene, to form the reactive α-oxo sulfine **17** *in situ* which is efficiently trapped with each of the nitrile oxides **12–16**.

Table 2 Cycloaddition to form the kinetic 1,2,5-oxathiazole-S-oxides

Entry	(Dipole)	Thermodynamic Product	Kinetic Product	Regioisomeric 1,4,2-oxathiazole-s-oxides	1,4,2-oxathiazole
					
1	Ratio	8	47	34	11
	R^1 = H(**12**)	**27**	**28** 6%	**29** 6%	**30** 9%
2	Ratio	14	68	7	0
	R^1 = 4-F(**13**)	**31**	**32** 28%	11% **33**	-
3	Ratio	0	80	20	0
	R^1 = 4-*t*Bu(**15**)	**34**	**35** 16%	**36**	-
4	Ratio	29	40	22	9
	R^1 = 4-NO_2(**14**)	**21**	**20** 24%	**22**	**23** 15%
5	Ratio	23	23	0	54
	R^1 = 2,5-difluoro(**16**)	**37**	**38**	-	**25** 8%

In Table 2, Entries 1-4 the targeted kinetic isomers were successfully isolated in each case, albeit in poor yields. Although the thermodynamic isomers were present in the ^{1}H NMR spectra of the crude product mixture, in this study the thermodynamic isomer was not isolated after purification in most instances. Significantly, while the selectivity for the kinetic isomer **20** over **21** was relatively modest, across the series of nitrile oxides formation of the kinetic cycloadducts **28**, **32** and **35** had a much higher selectivity. This may be due to slower interconversion of the cycloadducts and/or more efficient trapping of the *Z* sulfine with the nitrile oxides. Interestingly, the 1,4,2-oxathiazole-*S*-oxide regioisomers were present in four out of the five reactions in Table 3, whereas 1,4,2-oxathiazole was present in three of the five reactions. In the case of Table 2, entry 5, only the 1,4,2-oxathiazole **25** was isolated after repeated chromatography, in 8% yield. This 1,4,2-oxathiazole **25**, whose structure was confirmed by single crystal XRD, is a

reduction product; the deoxygenation of the sulfoxide may be effected by the rhodium catalyst or the intermediate carbene.[60] This set of reactions confirm that preferential formation of the kinetic isomer of 1,2,5-oxathiazole-*S*-oxides can be achieved using rhodium acetate dimer (5 mol %) at 0°C, and subsequently isolated and characterised as a pure compound in most cases (**20**, **28**, **32**, and **35**). On storage of each of these isomers, spontaneous interconversion to the thermodynamic isomers was observed over time (see below).

Isolation of Thermodynamic 1,2,5-oxathiazole-*S*-oxides.

With the optimum conditions in hand for the synthesis of the thermodynamically preferred stable cycloadducts (*i.e.* thermolysis in flow, Table 1, entry 8), the α-diazosulfoxides **1, 2** and **4** and substituted aryl nitrile oxide dipoles **12–16** were combined to generate a novel series of 1,2,5-oxathiazole-*S*-oxide cycloadducts in moderate yields (Table 3).

In each case, the thermodynamic 1,2,5-oxathiazole-*S*-oxide was the principal product formed and isolated as a pure component following chromatography. As summarised in Table 3, smaller amounts of the other cycloadducts were seen in the crude product mixtures including the kinetic 1,2,5-oxathiazole-*S*-oxide, the 1,4,2-oxathiazole-*S*-oxide regioisomers, and in some instances samples of these were isolated. Notably 1,4,2-oxathiazole was not formed under these conditions in any instance, indicating that the sulfoxide reduction only occurs in the presence of the rhodium catalyst.

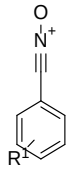
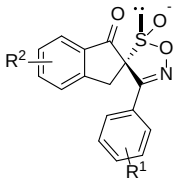
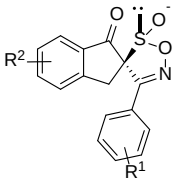
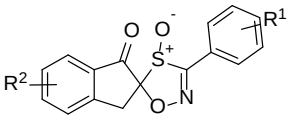
In all cases, as with the earlier reactions, the dipole was freshly generated each time and added as a solution in dichloromethane, to the α-diazosulfoxide and the mixture subjected to thermolysis under continuous flow. Under these conditions efficient transformation of the α-diazosulfoxide to the α-oxo sulfine is achieved. Trapping of the *Z* α-oxo sulfine to form the kinetic 1,2,5-oxathiazole-*S*-oxide and the *E* α-oxo sulfine to form the thermodynamic 1,2,5-oxathiazole-*S*-oxide cycloadduct can be envisaged, with subsequent transformation of the kinetic isomer to the thermodynamic isomer effected at 100°C.

Unambiguous confirmation of the regiochemistry and stereochemistry of a number of the thermodynamic 1,2,5-oxathiazole-*S*-oxides was undertaken by single crystal XRD (Figure 3).

Interestingly while across the series of compounds there is evidence that the kinetic 1,2,5-oxathiazole-*S*-oxide cycloadducts convert to the thermodynamic isomers, the rate of the interconversion varies depending on the substituents. In particular, ^{1}H NMR spectroscopy on a sample of the kinetic *t*-butyl derivative **35** following storage for 6 months as a solid showed that only a small amount had converted to the thermodynamic isomer **34**, while the analogous 4-fluoro derivative **32** converted to **31** to a much great extent following 5 months storage (see ESI for spectra). The entropic barrier to reorganisation of the sterically demanding t-butyl group in the solid state is evident.

Undertaking the cycloadditions in continuous flow offers many benefits leading to the thermodynamic 1,2,5-oxathiazole-*S*-oxides in a metal free and catalyst free transformation. In addition, the benefits of continuous flow processing result in an easily controlled thermolysis (rapid heating, excellent thermal transfer and efficient removal of the product from the hot zone once formed) and a readily scalable process.

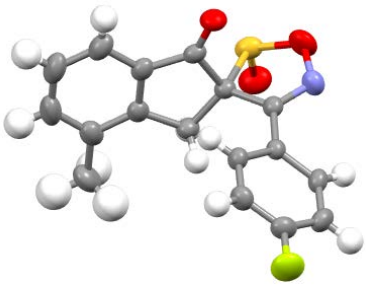
*Table 3: Dipolar cycloadditions in flow using a range of aryl nitrile oxides**

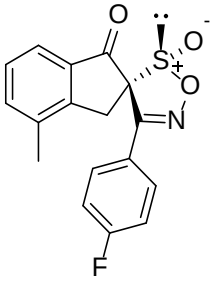
Entry	Dipole	Thermodynamic Product	Kinetic Product	Regioisomers
				
1	Ratio:	63	12	7,15
	R^1 = H, R^2 = H	**27** 32%	**28**	**39 , 29**
2	Ratio	78	12	10
	R^1 = 4-*t*Bu, R^2 = H	**34** 30%	**35**	**40** 5%
3	Ratio	63	18	12
	R^1 = 4-F, R^2 = H	**31** 35%	**32** 12%	**33** 4%
4	Ratio	56	10	14
	R^1 = 4-NO_2, R^2 = H	**21** 52%	**20**	**22**
5	Ratio	62	0	9
	R^1 = 2,5-diF, R^2 = H	**37** 11%	**38**	**41**
6	Ratio	78	18	8
	R^1 = H, R^2 = 2-Me	**42** 30%	**43**	**44**
7	Ratio	77	11	12
	R^1 = 4-F, R^2 = 2-Me	**45** 45%	46	**47** 12%
8	Ratio	78	15	7
	R^1 = 4-tBu, R^2 = 2-Me	**48** 26%	**49**	**50**
9	Ratio	85	11	4
	R^1 = 4-NO_2 R^2 = 2-Me	**51** 20%	**52**	**53**
10	Ratio	64	16	11
	R^1 = H, R^2 = 4-Me	**54** 34%	**55**	**56** 11%

11	Ratio R^1 = 4-F, R^2 = 4-Me	73 **57** 36%	14 **58** 5%	13 **59** 10%
12	Ratio R^1 = 4-tBu, R^2 = 4-Me	80 **60** 15%	20 **61**	0 -
13	Ratio R^1 = 4-NO_2, R^2 = 4-Me	77 **62** 45%	17 **63** 11%	6 **64**
14	Ratio R^1 = 2,5-DiF, R^2 = 4-Me	53 **65** 16%	11 **66**	0 -

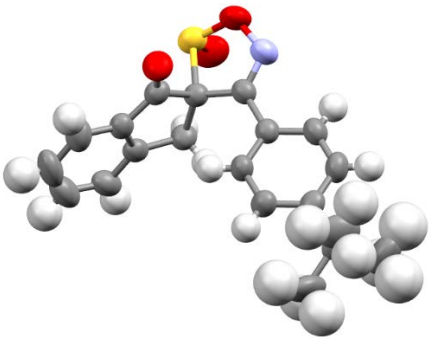
*Yields of pure compounds isolated after column chromatography on silica gel are given in the table. There was no notable change in the efficiency of the transformation over time.

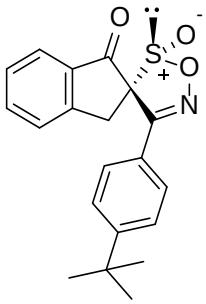
Crystal Structure **1,2,5-Oxathiazole-*S*-oxide**



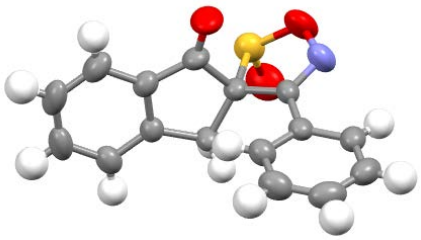


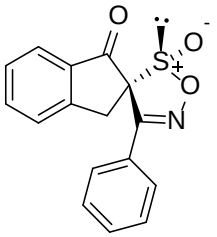
45





34





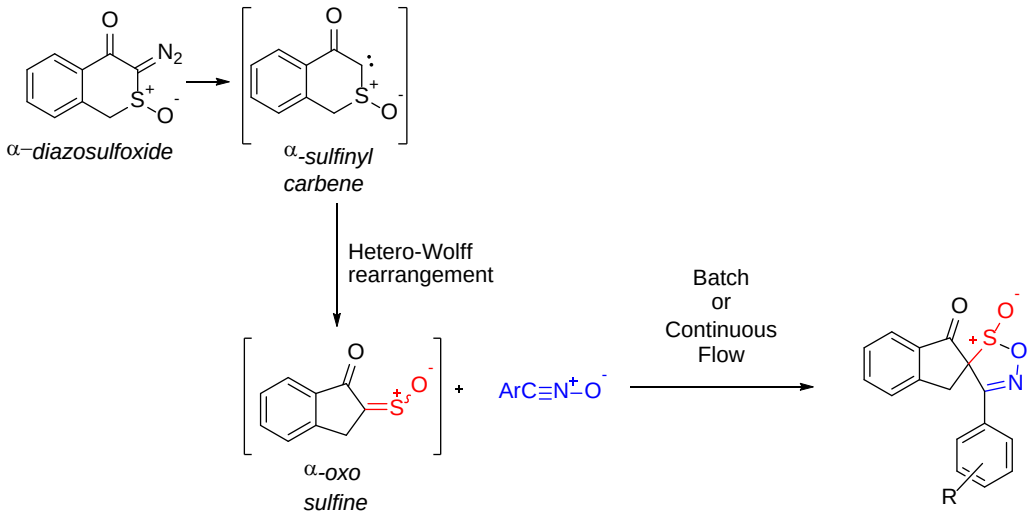
27

Figure 3: Confirmation of regiochemistry and stereochemistry for a range of thermodynamic 1,2,5-oxathiazole-S-oxides. Structures are displayed using the Mercury 2.7 package.

Exploiting the differences between use of a rhodium catalyst or thermolysis in flow, two sets of reaction conditions have been established to predictably lead to preferential formation of either the kinetic isomer or the thermodynamic isomer of a 1,2,5-oxathiazole-*S*-oxide cycloadducts through trapping of α-oxo sulfines with nitrile oxides. Most reports of nitrile oxide cycloadditions with sulfines, are to isolated sulfines, and yield the 1,4,2-oxathiazole-*S*-oxide regioisomer;[10] we are not aware of a nitrile oxide cycloaddition to an α-oxo sulfine. It is well established that the conjugation in an α-oxo sulfine alters the electronic properties and accordingly the reactivity of the sulfine moiety. In Zwanenburg's discussion of the regioselectivity of cycloaddition of α-oxo sulfines with Danishefsky's diene, the impact of the conjugation to the ketone on the orbital coefficients is highlighted. Thus in an isolated sulfine the largest atomic coefficient in the LUMO is on the carbon, while in the oxo-sulfine the polarisation is reversed with the largest coefficient now at sulfur.[61] The regiochemical outcome of the dipolar cycloadditions in this work can be similarly rationalised.

The key spectroscopic characteristics are consistent across the series of the compounds isolated. The majority of the thermodynamic isomers of the 1,2,5-oxathiazole-*S*-oxides are crystalline solids and the ^{13}C NMR shift of the carbon at the spiro centre is extremely consistent across the series, at 96.5 - 97.8 ppm, compared to 92.5 - 93.4 ppm for the kinetic 1,2,5-oxathiazole-*S*-oxide isomers. Furthermore, in each of the diastereomers the AB signals for the diastereotopic CH_2 are very distinctive in the ^{1}H NMR spectra, and are very consistent across the series. The formation of the 1,4,2-oxathiazole-*S*-oxide regioisomers, is evidenced by the signal for the spiro carbons at *ca*. 108 ppm in one regioisomer and *ca*. 110 ppm for the second regioisomer, deshielded relative to the corresponding signal in the 1,2,5-oxathiazole-*S*-oxides, due to proximity to oxygen. For the isolated examples of the 1,4,2-oxathiazoles, the shift of the spiro centre is consistently observed between a narrow range of 101.1 – 102.2 ppm in the ^{13}C NMR spectrum. Again, a crystal structure of the compound **25** was obtained during this work, unambiguously confirming the heterocyclic structure.

Overall, starting from α-diazosulfoxides, via α-sulfinyl carbene and α-oxo sulfine intermediates, we have generated a novel series of fourteen thermodynamic diastereomers and four kinetic diastereomers of 1,4,2-oxathiazole-*S*-oxide cycloadducts, with regiochemistry and stereochemistry confirmed in four cases by single crystal X-ray diffraction (Scheme 7). In addition, 1,4,2-oxathiazole-*S*-oxides are formed as minor regioisomeric by-products in these reactions.



Scheme 7

Conclusion

In summary, we have successfully established synthetic methodology for the generation of novel 1,2,5-oxathiazole-*S*-oxide cycloadducts, an interesting series of spirocyclic heterocycles, from cycloaddition of nitrile oxide dipoles with α-oxo sulfines generated in situ from α-diazosulfoxides. Through a reaction optimisation study, conditions for the isolation of the kinetic isomer were established using rhodium acetate as a catalyst at 0°C under traditional batch conditions, while using continuous flow thermolysis optimal conditions for the synthesis of the thermodynamic isomers were established. Based on biological activity seen in related heterocycles,[62-64] investigation of the biological activity of these novel heterocycles is underway and will be reported in due course.

Conflicts Of Interest

There are no conflicts of interest to declare.

Acknowledgements.

We thank The Irish Research Council (IRC) for financial support (PGM) (GOIPG/2013/244). We thank the Synthesis and Solid State Pharmaceutical Centre supported by the Science Foundation Ireland (grant: SFI SSPC2 12/RC/2275).and Science Foundation Ireland for equipment grant 05/PICA/B802/EC07).

Supplementary data

The supporting information is available free of charge at DOI XXXXXXXXXXXXXX containing: experimental procedures, and ^{1}H and ^{13}C NMR spectra. Crystal structures corresponding to those outlined above are available in the CCDC with the following codes:

21 : CCDC 1875539, **27**: CCDC 1875540, **34**: CCDC 1875541, **25**: CCDC 1875542, **45**: CCDC 1875543

Experimental

Representative procedure for reaction conditions for synthesis of the kinetic 1,2,5-oxathiazole-S-oxide as major product

The nitrile oxide dipole **12** was generated from the imidoyl chloride precursor (0.155 g, 1.00 mmol, 2.3 eq) as described in the ESI. The solution of dipole **12** was concentrated under reduced pressure and added to the α-diazosulfoxide **1** (0.090 g, 0.43 mmol, 1 eq) in dichloromethane/ethyl acetate (1 : 1, 15 mL). This was followed by the addition of rhodium acetate dimer (0.009 g, 0.02 mmol, 5 mol %). The reaction mixture was stirred at room temperature under a nitrogen atmosphere for 1 h. The crude reaction mixture was concentrated under reduced pressure to give the crude material as an orange oil. Analysis of the crude material by ^{1}H NMR spectroscopy showed no signals corresponding to either the α-diazosulfoxide **1**, or the intermediate α-oxo sulfine **17**. Purification of the reaction mixture by flash chromatography on silica gel using gradient hexane-ethyl acetate as eluent (100 : 0 – 60 : 40) led to the elution of multiple fractions. The first fraction to elute was the 1,4,2-oxathiazole **30** as a yellow crystalline solid (0.026 g, 9%); mp 89 – 90°C; ν_{max}/cm^{-1} (neat) 1719, 1273, 1083, 743; δ_H (400 MHz, $CDCl_3$); 3.79 (1H, d, *J* 18.0, A of AB_q, one of CH_2), 3.92 (1H, d, *J* 18.0, B of AB_q, one of CH_2), 7.40 – 7.52 (6H, m, 6 x Aromatic CH), 7.68 – 7.73 (2H, m, 2 x Aromatic CH), 7.89 (1H, d, *J* 7.6, 1 x Aromatic CH); δ_C ($CDCl_3$, 100 MHz); 42.7 (CH_2, $ArCH_2$), 101.1 (Cq, C_{spiro}), 125.8, 126.4 (CH, 2 x Aromatic CH), 127.5 (Cq, 1 x Aromatic Cq), 128.2 (CH, 2 x Aromatic CH), 128.7 (CH, 2 x Aromatic CH), 131.3 (CH, 1 x Aromatic CH), 132.6 (Cq, 1 x Aromatic Cq), 136.7 (CH, 1 x Aromatic CH), 149.2 (Cq, 1 x Aromatic Cq), 155.2 (Cq, C=N), 196.2 (Cq, C=O).

The second fraction was a mixture of thermodynamic isomer **27** and regiosiomer **29**, regio : thermodynamic, 0.73 : 1, **29** : **27**. The material was characterised as a mixture and spectral characteristics for the 1,4,2-oxathiazole-*S*-oxide Regioisomer **29** are; (0.023 g, 8%); ν_{max}/cm^{-1} (neat) 1714, 1367, 1154; δ_H (400 MHz, $CDCl_3$); 3.66 (1H, d, *J* 18.9, A of AB_q, one of CH_2), 4.28 (1H, d, *J* 18.4, B of AB_q, one of CH_2), 7.29 – 7.98 [multiple overlapping signals including (3H, m, 3 x ArH), (3H, m, 3 x Aromatic CH), (1H, m, 1 x Aromatic CH), (1H, m, 1 x Aromatic CH) and (1H, m, 1 x Aromatic CH)]; δ_C ($CDCl_3$, 100 MHz); 28.6 (CH_2, $ArCH_2$), 110.8 (Cq, C_{spiro}), 125.6 (Cq, Aromatic Cq), 125.7, 126.8 (CH, 2 x Aromatic CH), 127.6 (1 x Aromatic Cq), 128.7 (2 x Aromatic CH), 128.8 (1 x Aromatic CH), 129.5 (CH, 2 x Aromatic CH), 133.0 (Cq, Aromatic Cq), 137.1 (CH, Aromatic CH), 149.0 (Cq, Aromatic Cq), 158.7 (Cq, C=N), 193.2 (Cq, C=O); (M+H) 298 (30%); HRMS (ESI+) Exact mass calculated for $C_{16}H_{11}NO_3S$ $[M-H]^+$, 298.0538. Found: 298.0533. Signals corresponding to **27** are δ_H (400 MHz, $CDCl_3$) 3.49 (1H, d, *J* 19.2, A of AB_q, CH_2), 4.07 (1H, d, *J* 19.2, B of AB_q, CH_2), 7.29

– 7.60 (7H, m, 7 x Aromatic CH), 7.79 (1H, t, *J* 8.5, 1 x Aromatic CH), 7.96 (1H, d, *J* 7.8, 1 x Aromatic CH); δ_C ($CDCl_3$, 100 MHz); 28.9 (CH_2, $ArCH_2$), 97.4 (Cq, C_{spiro}), 125.6 (Cq, Aromatic Cq), 126.1, 127.0 (2 x CH, 2 x Aromatic CH), 128.0 (CH, 2 x Aromatic CH), 129.2, (CH, 1 x Aromatic CH), 129.4 (CH, 2 x Aromatic CH), 131.7 (CH, 1 x Aromatic CH), 134.3 (Cq, 1 x Aromatic Cq), 137.1 (CH, 1 x Aromatic CH), 151.6 (Cq, Aromatic Cq), 158.0 (Cq, C=N), 192.6 (Cq, C=O).

The third fraction contained the kinetic diastereomer **28** (0.014 g 6%). ν_{max}/cm^{-1} (neat) 1716, 1601, 1168, 760; δ_H (400 MHz, $CDCl_3$); 3.64 (1H, d, A of AB_q *J* 18.8, one of CH_2), 3.83 (1H, d, B of AB_q, *J* 18.2, one of CH_2), 7.34 – 8.10 [overlapping signals including (2H, t, *J* 7.6, 8.1, 2 x ArH), a (3H, m, 3 x Aromatic CH), a (2H, m, 2 x Aromatic CH), a (1H, t, *J* 7.3, 8.5, 1 x Aromatic CH) and (1H, d, *J* 7.8 1 x Aromatic CH).

4'-(4-(tert-Butyl)phenyl)spiro[indene-2,3'-[1,2,5]oxathiazol]-1*(3H)*-one *S*-oxide 35

Kinetic cycloadduct **35** was isolated as a white crystalline solid (0.040 g, 16%). Mp 128 – 129 °C; ν_{max}/cm^{-1} (neat) 753, 1165, 1712; δ_H (400 MHz, $CDCl_3$); 1.24 (9H, s, 3 x CH_3), 3.62 (1H, d, *J* 18.4, A of AB_q, one of $ArCH_2$), 3.81 (1H, d, *J* 18.4, B of AB_q, one of $ArCH_2$), 7.35 – 7.44 (4H, symmetrical q, *J* 8.7, 4 x Aromatic CH), 7.56 – 7.64 (2H, m, 2 x Aromatic CH), 7.80 (1H, t, *J* 7.5, 2 x Aromatic CH), 7.96 (1H, d, *J* 7.8, 1 x Aromatic CH); δ_C ($CDCl_3$, 100 MHz); 31.0 [CH_3, $C(CH_3)_3$], 32.0 (CH_2, $ArCH_2$), 35.0 [Cq, $C(CH_3)_3$], 93.4 (Cq, C_{spiro}), 122.3 (Cq, $CqCH_2$), 125.6 (CH, 1 x Aromatic CH), 126.3 (CH, 2 x Aromatic CH), 127.1 (CH, 1 x Aromatic CH), 128.0 (CH, 2 x Aromatic CH), 129.3 (CH, 1 x Aromatic CH), 136.6 (Cq, Aromatic Cq), 136.8 (CH, Aromatic CH), 149.2 (Cq, Aromatic Cq), 155.6 (Cq, Aromatic Cq-$C(CH_3)_3$), 158.8 (Cq, C=N), 191.0 (Cq, C=O); (M+H) 354 (10%); HRMS (ESI+) Exact mass calculated for $C_{20}H_{20}NO_3S$ $[M-H]^+$, 354.1164. Found: 354.1157.

4'-(4-Fluorophenyl)spiro[indene-2,3'-[1,2,5]oxathiazol]-1(3H)-one 2'-oxide 32

The first fraction contained the kinetic 1,2,5-oxathiazole-S-oxide **32** (0.045 g, 28%) Yellow oily residue; Found C, 60.54; H 3.40 N 4.30. $C_{16}H_{10}NFO_3S$ requires C, 60.95; H 3.20 ; N 4.44; ν_{max}/cm^{-1} (neat) 1716, 1602, 1508, 1160; δ_H (400 MHz, $CDCl_3$) 3.60 (1H, d, A of AB_q *J* 18.3, one of $ArCH_2$), 3.83 (1H, d, B of AB_q, *J* 18.3, one of $ArCH_2$), 7.04 (2H, t, *J* 8.6, 2 x Aromatic CH), 7.46 – 7.49 (2H, m, 2 x Aromatic CH), 7.58 – 7.65 (2H, m, 2 x Aromatic CH), 7.82 (1H, t, *J* 7.4, 1 x Aromatic CH), 7.96 (1H, d, *J* 7.7, 1 x Aromatic CH); δ_C ($CDCl_3$, 100 MHz); 31.8 (CH_2, $ArCH_2$), 93.2 (Cq, C_{spiro}), 116.7 (CH, 2 x Aromatic CH, d, $^2J_{CF}$ 22.3), 121.6 (Cq, d, $^4J_{CF}$ 3.5, 1 x Aromatic Cq), 125.7, 127.2, 129.5 (CH, 3 x Aromatic CH), 130.4 (CH, 2 x ArCH, d, $^3J_{CF}$ 9) ,136.4 (Cq, 1 x Aromatic Cq), 137.0 (CH, 1 x Aromatic CH), 149.0 (Cq, 1 x Aromatic Cq), 158.0 (Cq, C=N), 164.7 (CF, Aromatic CF, d, $^1J_{CF}$ 254.6), 190.8 (Cq, C=O).The second fraction to elute contained the 1,4,2-oxathiazole-*S*-oxide Regioisomer **33** (0.018 g, 11%) Pale yellow crystalline solid; mp 159 - 161°C; ν_{max}/cm^{-1} (neat) 1721, 1073, 844; δ_H (400 MHz, $CDCl_3$) 3.33 (1H, d, *J* 17.2, A of AB_q, one of $ArCH_2$), 3.51 (1H, d, *J* 17.2, B of AB_q, one of $ArCH_2$), 7.18 – 7.24 (3H, m, 3 x Aromatic CH), 7.51 – 7.58 (2H, m, 2 x Aromatic CH), 7.77 (1H, t, *J* 8.7, 2 x Aromatic CH), 7.93 – 7.98 (2H, m, 2 x Aromatic CH); δ_C ($CDCl_3$, 100 MHz) 33.6 (CH_2, $ArCH_2$), 108.3 (Cq, C_{spiro}), 117.0 (CH, 2 x Aromatic CH, d, $^2J_{CF}$ 22), 125.6, 127.1, 129.4 (CH, 3 x Aromatic CH), 131.0 (CH, 2 x ArCH, d, $^2J_{CF}$ 9), 135.2 (Cq, 1 x Aromatic Cq), 137.1 (CH, 1 x Aromatic CH), 147.4 (Cq, 1 x Aromatic Cq), 158.4 (Cq, C=N), 188.9 (Cq, C=O).The C_F bond was not observed in the ^{13}C NMR spectrum.

4'-(2,5-Difluorophenyl)spiro[indene-2,3'-[1,2,5]oxathiazol]-1(*3H*)-one 25

Only 1,4,2-oxathiazole **25** was isolated, as a pale yellow crystalline solid (0.018 g, 8%). mp 89 – 91°C; ν_{max}/cm^{-1} (neat) 1726, 1483, 1272; δ_H (400 MHz, $CDCl_3$) 3.78 (1H, d, *J* 18.0, A of AB_q, one of $ArCH_2$), 3.91 (1H, d, *J* 18.0, B of AB_q, one of $ArCH_2$), 7.10 – 7.19 (2H, m, 2 x Aromatic CH), 7.46 – 7.50 (2H, m, 2 x Aromatic CH), 7.57 – 7.61 (1H, m, 1 x Aromatic CH), 7.72 (1H, t, *J* 8.5, 1 x Aromatic CH), 7.88 (1H, d, *J* 7.6, 1 x Aromatic CH); δ_C ($CDCl_3$, 100 MHz) 42.5 (CH_2, $ArCH_2$), 101.1 (Cq, C_{spiro}), 115.8 (CH dd, $^2J_{CF}$ 26.0, $^3J_{CF}$ 3.0, 1 x Aromatic CH), 117.0 (Cq, dd, $^2J_{CF}$ 14.6, $^3J_{CF}$ 9.0, 1 x Aromatic Cq), 117.7 (CH, dd, $^2J_{CF}$ 25.5, $^3J_{CF}$ 8.7, 1 x Aromatic CH), 119.5 (CH, dd, $^2J_{CF}$ 25.5, $^3J_{CF}$ 8.8, 1 x Aromatic CH), 125.9. 126.4, 128.9 (CH, 3 x Aromatic CH), 132.4 (Cq, 1 x Aromatic Cq), 136.8 (CH, 1 x Aromatic CH), 148.8 (Cq, 1 x Aromatic Cq), 149.3 (Cq, C=N), 155.8 (Cq, 1 x Aromatic CF, d, $^1J_{CF}$ 251), 158.3 (Cq, 1 x Aromatic CF, d, $^1J_{CF}$ 245), 196.0 (Cq, C=O); m/z (ESI+) 334 $[M+H]^+$ (25%); HRMS (ESI+) Exact mass calculated for $C_{16}H_{10}NO_3F_2S$ $[M+H]^+$, 334.0349 Found: 334.0345. The relative stereochemistry of the cycloadduct **25** was determined by single crystal X-ray diffraction on a crystalline sample of **25** recrystallized from dichloromethane/hexane. Crystals of **25** are monoclinic, space group *P* 21/*c*. Crystal data for $C_{16}H_9F_2NO_2S$, *Mr* = 317.30, a = 14.0083 (10) Å, b = 8.7108 (6) Å, c = 11.54178 (8) Å, $\alpha = \gamma = 90$ °C, $\beta = 105.733$ (2)°, *V* = 1355.62 (16) Å^3, *Z* = 4, $D_c = 1.555$ g cm^{-3}, $F_{000} = 648$, Cu Kα radiation, λ = 1.541 Å, *T* = 296 K, $2\theta_{max} = 0.753$°, μ = 2.417 mm^{-1},15370 reflections collected, 2344 unique ($R_{int} = 0.0332$), final GooF = 1.100, $R_1 = 0.0328$, w$R_2 = 0.0920$ (2299 obs. data: $I > 2\sigma(I)$); $R_1 = 0.0335$, wR_2 = 0.0927 (all data).

(2R,2'R)-4'-(4-nitrophenyl)spiro[indene-2,3'-[1,2,5]oxathiazol]-1(3H)-one 2'-oxide 20

The first fraction to elute was the 1,4,2-oxathiazole **23** (0.031 g, 15%); mp 175 – 177°C; ν_{max}/cm^{-1} (neat) 1715, 1597, 1518; δ_H (400 MHz, $CDCl_3$) 3.82 (1H, d, *J* 17.9, A of AB_q, one of $ArCH_2$), 3.95 (1H, d, *J* 17.9, B of AB_q, one of $ArCH_2$), 7.48 – 7.53 (2H, m, 2 x Aromatic CH), 7.72 – 7.76 (1H, m, 1 x Aromatic CH), 7.87 – 7.91 (3H, m, 3 x Aromatic CH), 8.30 (2H, d, *J* 7.8, 2 x Aromatic CH); δ_C ($CDCl_3$, 100 MHz) 42.3 (CH_2, $ArCH_2$), 102.2 (Cq, C_{spiro}), 124.1 (CH, 2 x Aromatic CH), 126.0, 126.4 (CH, 2 x Aromatic CH), 128.9 (CH, 2 x Aromatic CH), 129.1 (CH, 1 x Aromatic CH), 131.2 (Cq, Aromatic Cq), 132.2 (Cq, Aromatic Cq), 133.4 (Cq, Aromatic Cq), 137.0 (CH, 1 x Aromatic CH), 149.1 (Cq, Aromatic Cq), 153.3 (Cq, C=N), 195.6 (Cq, C=O). The more polar second fraction to elute was the kinetic isomer **20** (0.048 g, 24%); mp 168 - 170°C; ν_{max}/cm^{-1} (neat) 1711, 1517; δ_H (400 MHz, $CDCl_3$) 3.61 (1H, d, *J* 18.3, A of AB_q, one of $ArCH_2$), 3.88 (1H, d, *J* 18.3, B of AB_q, one of $ArCH_2$), 7.62 (2H, t, *J* 8.3, 2 x Aromatic CH), 7.67 (2H, d, *J* 8.8, 2 x Aromatic CH_2, 7.81 – 7.89 (1H, m, 1 x Aromatic CH), 7.97 (1H, d, *J* 7.6, 1 x Aromatic CH), 8.21 (2H, d, *J* 8.9, 2 x Aromatic CH); δ_C ($CDCl_3$, 100 MHz) 31.5 (CH_2, $ArCH_2$), 92.5 (Cq, C_{spiro}), 124.4 (CH, 2 x Aromatic CH), 125.9, 127.2 (CH, 2 x Aromatic CH), 129.2 (CH, 2 x Aromatic CH), 129.8 (CH, 1 x Aromatic CH), 131.6, 136.2 (Cq, 2 x Aromatic Cq), 137.3 (CH, 1 x Aromatic CH), 148.8 (Cq, 1 x Aromatic Cq), 149.4 (Cq, 1 x Aromatic Cq), 157.5 (Cq, C=N), 190.4 (Cq, C=O).

Representative procedure for reaction conditions for synthesis of the thermodynamic 1,2,5-oxathiazole-S-oxide as major product

* In general, flow reactions were conducted using a Vapourtec E-Series reactor (Vapourtec V3 peristaltic pumps), solution was pumped through a 10 mL reaction coil (Vapourtec part number 50-1011) heated to 100°C at a rate of 1 mL/min giving a residence time of 10 min, followed by a 10 mm id Omnifit™ glass column (Vapourtec part number 30-3296) packed with Alumina (volume ~ 1 mL). PFA tubing was used throughout the system. The reaction mixture passed through a fixed 7 bar back pressure regulator (Kinesis part no. P-787), the crude material was collected as an orange solution and concentrated under reduced pressure.

(2S,2'R)-4'-(4-nitrophenyl)spiro[indene-2,3'-[1,2,5]oxathiazol]-1(3H)-one 2'-oxide 21

The imidoyl chloride **67** (0.278 g, 1.38 mmol, 2.3 eq) was added portionwise over 10 min, at room temperature to a vigorously stirred solution of aqueous NaOH (1M, 10 mL) and dichloromethane (10 mL). After complete addition, the mixture was stirred for a further 10 min. The layers were separated, and the organic layer was dried with anhydrous $MgSO_4$ and concentrated under reduced pressure. After concentration *in vacuo* the dipole **14** was isolated as a white solid and dissolved in ethyl acetate/dichloromethane (1 : 1, 5 mL). The α-diazosulfoxide **1** (0.105 g, 0.51 mmol, 1 eq) was dissolved in ethyl acetate/dichloromethane (1 : 1, 5 mL) and subsequently added to the solution of the dipole **14**. Using a Vapourtec E-Series reactor (peristaltic pumps), this solution was pumped through a 10 mL reaction coil heated to 100°C at a rate of 1 mL/min giving a residence time of 10 min, followed by a 10 mm id Omnifit™ glass column packed with Alumina (volume ~ 1 mL).[35] The reaction mixture passed through a 7 bar back pressure regulator (Kinesis part no. P-787), the crude material was collected as an orange solution and concentrated under reduced pressure to give the crude product as an orange crystalline solid (0.195 g). Analysis by ^{1}H NMR spectroscopy showed the material to be a mixture of the thermodynamic (**21**) and kinetic (**20**) cycloadducts along with a regioisomer (**22**) and an unknown impurity (56 : 10 : 14 : 30). The crude material was purified by trituration with ether and isolation of a crop of the thermodynamic isomer **21** was achieved as an off white crystalline solid (0.089 g, 52%). In some instances, the crude reaction mixture was dissolved in the minimum amount of dichloromethane, and purified by column chromatography on silica gel using gradient hexane-ethyl acetate as eluent (100 : 0 – 50 : 50).

White crystalline solid (0.089 g, 52%) ; mp 159-161°C; ν_{max}/cm^{-1} (neat) 1699, 1522, 1345; δ_H (400 MHz, $CDCl_3$) 3.42 (1H, d, *J* 19.3, A of AB_q, CH_2), 4.12 (1H, d, *J* 19.3, B of AB_q, CH_2), 7.52 (2H, d, *J* 8.9, 2 x ArH on $ArNO_2$), 7.62 (2H, t, *J* 8.2, 7.2 2 x Aromatic CH), 7.84 (1H, t, *J* 7.4, 8.4, 1 x Aromatic CH), 7.99 (1H, d, *J* 7.7, 1 x Aromatic CH) 8.23 (2H, d, *J* 8.9, 2 x ArH on $ArNO_2$); δ_C ($CDCl_3$, 100 MHz) 28.4 (CH_2, $ArCH_2$), 96.6 (Cq, C_{spiro}), 124.5 (CH, 2 x Aromatic CH), 126.3, 127.1 (CH, 2 x Aromatic CH), 129.1 (CH, 2 x Aromatic CH), 129.6 (CH, Aromatic CH), 131.9, 134.0 (Cq, 2 x Aromatic Cq), 137.5 (CH, 1 x Aromatic CH), 149.5, 151.2 (Cq, 2 x Aromatic Cq), 156.5 (Cq, C=N), 192.0 (Cq, C=O). HRMS (ESI+) Exact mass calculated for $C_{16}H_{11}N_2O_5S$ $[M+H]^+$, 343.0389. Found: 343.0388. The relative stereochemistry of the thermodynamic isomer **21** was established by single crystal X-ray diffraction on a crystal grown by slow recrystallization from dichloromethane and toluene over 4 - 5 weeks. Crystal data for **21**: $C_{16}H_{10}N_2OS$, *Mr* = 342.32 , triclinic *P*-1, a = 7.5520(11) Å, b = 8.2283(11) Å, c = 12.8010(18) Å, a = 74.726 (4), β =86.674 (5)°, g = 72.819 (4) *V* = 732.95 (18) Å^3, *Z* = 2, D_c = 1.55 g cm^{-3}, F_{000} = 352, Mo Kα radiation, λ = 0.7107 Å, *T* = 300(2) K, $2\theta_{max}$ = 26.40°, μ = 0.252 mm^{-1}, 15211 reflections collected, 2275 unique (R_{int} = 0.0445), final GooF = 1.054, R_1 = 0.0510, wR_2 = 0.1583 (2275 obs. data: $I > 2\sigma(I)$); R_1 = 0.0643, wR_2 = 0.1729 (all data).

(2S,2'R)-4'-Phenylspiro[indene-2,3'-[1,2,5]oxathiazol]-1(3H)-one 2'-oxide 27

White crystalline solid (0.089 g, 32%). Found C, 64.41; H 3.91; N 4.77. $C_{16}H_{11}NO_3S$ requires C, 64.63; H 3.73 ; N 4.71; mp 101-102°C; ν_{max}/cm^{-1} (neat) 1713, 1157; δ_H (400 MHz, $CDCl_3$) 3.49 (1H, d, *J* 19.2, A of AB_q, CH_2), 4.07 (1H, d, *J* 19.2, B of AB_q, CH_2), 7.29 – 7.60 (7H, m, 7 x Aromatic CH), 7.79 (1H, t, *J* 8.5, 1 x Aromatic CH), 7.96 (1H, d, *J* 7.8, 1 x Aromatic CH); δ_C ($CDCl_3$, 100 MHz); 28.9 (CH_2, $ArCH_2$), 97.4 (Cq, C_{spiro}), 125.6 (Cq, Aromatic Cq), 126.1, 127.0 (2 x CH, 2 x Aromatic CH), 128.0 (CH, 2 x Aromatic CH), 129.2, (CH, 1 x Aromatic CH), 129.4 (CH, 2 x Aromatic CH), 131.7 (CH, 1 x Aromatic CH), 134.3 (Cq, 1 x Aromatic Cq), 137.1 (CH, 1 x Aromatic CH), 151.6 (Cq, Aromatic Cq), 158.0 (Cq, C=N), 192.6 (Cq, C=O); HRMS (ESI+) Exact mass calculated for $C_{16}H_{10}NO_3S$ $[M-H]^+$, 296.0381. Found: 296.0375. The relative stereochemistry of the cycloadduct **27** was determined by single crystal X-ray diffraction on a crystalline sample of **27** recrystallized from dichloromethane/hexane. Crystals of **27** are triclinic, space group *P* -1. Crystal data for $C_{16}H_{11}NO_3S$, *Mr* = 297.32, a = 7.342 (2) Å, b = 8.954 (3) Å, c = 11.714 (3) Å, α = 70.226 (9)°, β = 83.607 (9)°, γ = 72.230 (9), *V* = 960.1 (3) Å^3, *Z* = 2, D_c = 1.431 g cm^{-3}, F_{000} = 308, Mo Kα radiation, λ = 0.710 Å, *T* = 300 K, $2\theta_{max}$ = 1.000°, μ = .243 mm^{-1}, 6640 reflections collected, 2407 unique (R_{int} = 0.0360), final GooF = 1.055, R_1 = 0.0405, wR_2 = 0.1080 (1976 obs. data: $I > 2\sigma(I)$); R_1 = 0.0503, wR_2 = 0.1166 (all data).

(2S,2'R)-4'-(4-(tert-Butyl)phenyl)spiro[indene-2,3'-[1,2,5]oxathiazol]-1(3H)-one 2'-oxide 34

The first fraction contained the thermodynamic isomer **34** (0.066 g, 30%); as a yellow crystalline solid; mp 119 – 120°C; ν_{max}/cm^{-1} (neat) 2961, 1712, 1267, 1149; δ_H(400 MHz, $CDCl_3$) 1.29 (9H, s, 3 x CH_3), 3.54 (1H, d, *J* 19.4, A of AB_q, one of $ArCH_2$), 4.08 (1H, d, *J* 19.4, B of AB_q, one of $ArCH_2$), 7.22 – 7.26 (2H, m, 2 x Aromatic CH), 7.35 – 7.37 (2H, m, 2 x Aromatic CH), 7.56 – 7.59 (2H, m, 2 x Aromatic CH), 7.79 (1H, t, *J* 8.5, 1 x Aromatic CH), 7.96 (1H, d, *J* 7.8, 1 x Aromatic CH); δ_C ($CDCl_3$, 100 MHz); 29.0 (CH_2, $ArCH_2$), 31.0 (CH_3, 3 x CH_3), 35.0 [Cq, $Cq(CH_3)_3$], 97.5 (Cq, C_{spiro}), 122.6 (Cq, Aromatic Cq), 126.1 (CH, 1 x Aromatic CH), 126.4 (CH, 2 x Aromatic CH), 127.0 (CH, 1 x Aromatic CH), 127.8 (CH, 2 x Aromatic CH), 129.1 (CH, 1 x Aromatic CH), 134.3 (Cq, Aromatic Cq), 137.0 (CH, Aromatic CH), 151.7 (Cq, Aromatic Cq), 155.4 (Cq, Aromatic Cq), 157.8 (Cq, C=N), 192.7 (Cq, C=O); HRMS (ESI+) Exact mass calculated for $C_{20}H_{20}NO_3S$ $[M+H]^+$, 354.1164. Found: 354.1169. The relative stereochemistry of the cycloadduct **34** was determined by single crystal X-ray diffraction on a crystalline sample of **34** recrystallized from dichloromethane/hexane. Crystals of **34** are monoclinic, space group *P* 21/*c*. Crystal data for $C_{20}H_{19}NO_3S$, *Mr* = 353.42, a = 11 .0131 (2) Å, b = 11.9246 (2) Å, c = 14.5681 (3) Å, α = γ = 90 °C, β = 107.106 (10)°, *V* = 1828.55 (6) Å^3, *Z* = 4, D_c = 1.284 g cm^{-3}, F_{000} = 744, Cu Kα radiation, λ = 1.541 Å, *T* = 296 K, $2\theta_{max}$ = 0.750°, μ = 1.721 mm^{-1}, 22017 reflections collected, 3172 unique (R_{int} = 0.0256), final GooF = 1.060, R_1 = 0.0549, wR_2 = 0.1588, (3041 obs. data: $I > 2\sigma(I)$); R_1 = 0.0562, wR_2 = 0.1600 (all data). The second fraction to elute contained the 1,4,2-oxathiazole-*S*-oxide regioisomer **40** (0.011 g, 5%) Yellow oil. ν_{max}/cm^{-1} (neat) 2962, 1726, 1272, 1083; δ_H (400 MHz, $CDCl_3$) 1.33 (9H, s, 3 x CH_3), 3.31 (1H, d, *J* 17.3, A of AB_q, one of $ArCH_2$), 3.47 (1H, d, *J* 17.3, B of AB_q, one of $ArCH_2$), 7.74 – 7.57 (4H, m, 4 x Aromatic CH), 7.76 (1H, t, *J* 7.8, 1 x Aromatic CH), 7.87 (2H, d, *J* 7.8, 2 x Aromatic CH), 7.97 (1H, d, *J* 7.8, 1 x Aromatic CH); δ_C ($CDCl_3$, 100 MHz); 31.0 (CH_3, 3 x CH_3), 33.6 (CH_2, $ArCH_2$), 35.2 [Cq, $Cq(CH_3)_3$], 107.9 (Cq, C_{spiro}), 122.1 (Cq, Aromatic Cq), 125.5 (CH, 1 x Aromatic CH), 126.7 (CH, 2 x Aromatic CH), 127.1, (CH, 1 x Aromatic CH), 128.8 (CH, 2 x Aromatic CH), 129.3 (CH, 1 x Aromatic CH), 135.3 (Cq, 1 x Aromatic Cq), 137.0 (CH, 1 x Aromatic CH), 147.5 (Cq, 1 x Aromatic Cq), 156.0 (Cq, 1 x Aromatic Cq), 159.4 (Cq, C=N), 189.2 (Cq, C=O); HRMS (ESI+) Exact mass calculated for $C_{20}H_{20}NO_3S$ $[M+H]^+$, 354.1164. Found: 354.1175.

(2S,2'R)-4'-(4-Fluorophenyl)spiro[indene-2,3'-[1,2,5]oxathiazol]-1(3H)-one 2'-oxide 31

The first fraction contained the thermodynamic isomer **31** (0.070, 35%) as a yellow crystalline solid; Found C, 60.45; H 3.30 N 4.73. $C_{16}H_{10}NFO_3S$ requires C, 60.95; H 3.20 ; N 4.44; mp 107 - 109°C; ν_{max}/cm^{-1} (neat) 3073, 1715, 1154; δ_H (400 MHz, $CDCl_3$) 3.45 (1H, d, *J* 19.2, A of AB_q, one of $ArCH_2$), 4.08 (1H, d, *J* 19.2, B of AB_q, one of $ArCH_2$), 7.05 (2H, t, *J* 8.6, 2 x Aromatic CH), 7.29 – 7.33 (2H, m, 2 x Aromatic CH), 7.59 (2H, t, *J* 8.5, 2 x Aromatic CH), 7.80 (1H, t, *J* 8.9, 1 x Aromatic CH), 7.98 (1H, d, *J* 7.5, 1 x Aromatic CH); δ_C ($CDCl_3$, 100 MHz) 28.8 (CH_2, $ArCH_2$), 97.2 (Cq, C_{spiro}), 116.8 (CH, 2 x Aromatic CH, d, $^2J_{CF}$ 22), 121.8 (Cq, d, $^4J_{CF}$ 3.6, 1 x Aromatic Cq), 126.2, 127.1, 129.3 (CH, 3 x Aromatic CH), 130.2 (CH, 2 x ArCH, d, $^3J_{CF}$ 8), 134.1 (Cq, 1 x Aromatic Cq), 137.3 (CH, 1 x Aromatic CH), 151.5 (Cq, 1 x Aromatic Cq), 157.0 (Cq, C=N), 164.7 (Cq, 1 x Aromatic CF, d, $^1J_{CF}$ 257), 192.5 (Cq, C=O). $(M+H)^+$ 316 (10%); HRMS (ESI+) Exact mass calculated for $C_{16}H_{11}NO_3FS$ $[M+H]^+$, 316.0444. Found: 316.0447. The second

fraction contained the kinetic isomer **32** (0.023 g, 12%) Yellow oily residue; ν_{max}/cm^{-1} (neat) 1716, 1602, 1510, 1160; δ_H (400 MHz, $CDCl_3$) 3.60 (1H, d, *J* 18.5, A of AB_q, one of $ArCH_2$), 3.83 (1H, d, *J* 18.0, B of AB_q, one of $ArCH_2$), 7.04 (2H, t, *J* 8.6, 2 x Aromatic CH), 7.46 – 7.50 (2H, m, 2 x Aromatic CH), 7.58 – 7.65 (2H, m, 2 x Aromatic CH), 7.82 (1H, t, *J* 8.2, 1 x Aromatic CH), 7.96 (1H, d, *J* 7.7, 1 x Aromatic CH); δ_C ($CDCl_3$, 100 MHz) 31.8 (CH_2, $ArCH_2$), 93.2 (Cq, C_{spiro}), 116.7 (CH, 2 x Aromatic CH, d, $^2J_{CF}$ 21), 121.6 (Cq, d, $^4J_{CF}$ 3.6, 1 x Aromatic Cq), 125.7, 127.1, 129.5 (CH, 3 x Aromatic CH), 130.4 (CH, 2 x Aromatic CH, d, $^3J_{CF}$ 8.6), 136.4 (Cq, 1 x Aromatic Cq), 136.9 (CH, 1 x Aromatic CH), 149.0 (Cq, 1 x Aromatic Cq), 158.0 (Cq, C=N), 164.7 (Cq, 1 x Aromatic CF, d, $^1J_{CF}$ 255), 190.7 (Cq, C=O); MS: $(M+H)^+$ 316 (10%); HRMS (ESI+) Exact mass calculated for $C_{16}H_{11}NO_3FS$ $[M+H]^+$, 316.0444. Found: 316.0444. The third fraction to elute was the 1,4,2-oxathiazole-*S*-oxide regiosiomer **33** as a yellow crystalline solid (0.08 g, 4%); ν_{max}/cm^{-1} (neat) 1725, 1601, 1238. 1082; δ_H (400 MHz, $CDCl_3$) 3.33 (1H, d, *J* 17.0, A of AB_q, one of $ArCH_2$), 3.51 (1H, d, *J* 17.2, B of AB_q, one of $ArCH_2$), 7.19 – 7.24 (3H, m, 3 x Aromatic CH), 7.51 – 7.58 (2H, m, 2 x Aromatic CH), 7.78 (2H, t, *J* 8.5, 2 x Aromatic CH), 7.93 – 7.98 (2H, m, 2 x Aromatic CH); δ_C ($CDCl_3$, 100 MHz)*; 33.6 (CH_2, $ArCH_2$), 108.4 (Cq, C_{spiro}), 117.1 (CH, d, $^2J_{CF}$ 21, 2 x Aromatic CH), 125.6, 127.1 129.4 (CH, 3 x Aromatic CH), 131.0 (CH, d, $^3J_{CF}$ 9.2, 2 x Aromatic CH), 137.2 (CH, 1 x Aromatic CH), 147.4 (Cq, 1 x Aromatic Cq); MS: (M+H) 316 (15%); HRMS (ESI+) Exact mass calculated for $C_{16}H_{11}NO_3FS$ $[M+H]^+$, 316.0444. Found: 316.0454. **Note:***The C=O, C-F, one Aromatic Cq, and the C=N signal were not detected in the ^{13}C NMR spectrum.

(2S,2'R)-4'-(2,5-Difluorophenyl)spiro[indene-2,3'-[1,2,5]oxathiazol]-1(3H)-one 2'-oxide 37

Careful and repeated chromatography was required for isolation of the thermodynamic isomer as a yellow oily residue (0.026 g, 11%). ν_{max}/cm^{-1} (neat) 1720, 1162, 1429; δ_H (400 MHz, $CDCl_3$) 3.37 (1H, d, *J* 18.8, A of AB_q, one of $ArCH_2$), 3.99 (1H, d, *J* 18.8, B of AB_q, one of $ArCH_2$), 6.99 – 7.04 (1H, complex m, 1 x Aromatic CH), 7.18 – 7.23 (1H, m, 1 x Aromatic CH), 7.76 (3H, t, *J* 8.9, 2 x Aromatic CH), 7.74 (1H, t, *J* 8.7, 1 x Aromatic CH), 7.92 (1H, d, *J* 7.6, 1 x Aromatic CH); δ_C ($CDCl_3$, 100 MHz) 28.3 (CH_2, $ArCH_2$), 97.1 (Cq, C_{spiro}), 115.3 (CH, dd, $^2J_{CF}$ 15.7, $^3J_{CF}$ 8.9, Aromatic C-3), 117.8 (CH, dd, $^2J_{CF}$ 24.7, $^3J_{CF}$ 8.5, Aromatic C-6), 118.1 (CH, dd, $^2J_{CF}$ 26.3, $^3J_{CF}$ 3.3, Aromatic C-4), 120.6 (CH, dd, $^2J_{CF}$ 24.1, $^3J_{CF}$ 9.1, Aromatic C-1), 125.9. 126.6, 128.9 (CH, 3 x Aromatic CH), 134.1 (Cq, 1 x Aromatic Cq), 136.5 (CH, 1 x Aromatic CH), 151.1 (Cq, 2 x Aromatic Cq), 154.4 (Cq, C=N), 156.3 (Cq, dd, $^1J_{CF}$ 251.3, $^4J_{CF}$ 5.9, 1 x C-F), 158.7 (Cq, d, $^1J_{CF}$ 244.8, 1 x C-F), 191.1 (Cq, d, $^5J_{CF}$ 4.2, C=O); MS (M^+) 333 (15%); HRMS (ESI+) Exact mass calculated for $C_{16}H_{10}NO_3F_2S$ $[M+H]^+$, 334.0360 Found: 334.0349.

4-Methyl-4'-phenylspiro[indene-2,3'-[1,2,5]oxathiazol]-1(*3H*)-one *S*-oxide 42

White crystalline solid (0.089 g, 30%). The first fraction contained the 1,2,5-oxathiazole-*S*-oxide thermodynamic isomer **42**; m.p. 150 – 151°C; ν_{max}/cm^{-1} (neat) 1709, 1156, 762; δ_H (400 MHz, $CDCl_3$) 2.38 (3H, s, CH_3), 3.32 (1H, d, *J* 19.0, A of AB_q, one of $ArCH_2$), 3.98 (1H, d, *J* 19.2, B of AB_q, one of $ArCH_2$), 7.29 – 7.31 (2H, m, 2 x Aromatic CH), 7.36 (2H, t, *J* 8.4, 2 x Aromatic CH), 7.46 – 7.51 (2H, m, 2 x Aromatic CH), 7.59 (1H, d, *J* 7.3, 1 x Aromatic CH), 7.80 (1H, d, *J* 7.6, 1 x Aromatic CH); δ_C ($CDCl_3$, 100 MHz) 17.8 (CH_3, $ArCH_3$), 27.9 (CH_2, $ArCH_2$), 97.4 (Cq, C_{spiro}), 123.5 (CH, 1 x Aromatic CH), 125.7 (Cq, 1 x Aromatic Cq), 127.9 (CH, 2 x Aromatic CH), 129.3 (CH, 1 x Aromatic CH), 129.4 (CH, 2 x Aromatic CH), 131.7 (CH, 1 x Aromatic CH), 134.1 (Cq, 1 x Aromatic Cq), 136.6 (Cq, 1 x Aromatic Cq), 137.7 (CH, 1 x Aromatic CH), 150.5 (Cq, 1 x Aromatic Cq), 158.0 (Cq, C=N), 192.8 (Cq, C=O); $(M)^+$ 311 (5%); HRMS (ESI+) Exact mass calculated for $C_{17}H_{14}NO_3S$ $[M+H]^+$, 312.0694. Found: 312.0687.

4'-(4-Fluorophenyl)-4-methylspiro[indene-2,3'-[1,2,5]oxathiazol]-1(*3H*)-one *S*-oxide 45

The first fraction isolated contained the thermodynamic isomer **45** as a white crystalline solid (0.098 g, 45%); mp 147 - 149°C, ν_{max}/cm^{-1} (neat) 1714, 1232, 1154; δ_H (400 MHz, $CDCl_3$) 2.39 (3H, s, CH_3), 3.28 (1H, d, *J* 19.2, A of AB_q, one of CH_2), 3.98 (1H, d, *J* 19.2, B of AB_q, one of CH_2), 7.06 (2H, t, *J* 8.6, 2 x Aromatic CH), 7.29 – 7.33 (2H, m, 2 x Aromatic CH), 7.50 (1H, t, *J* 7.8, 1 x Aromatic CH), 7.60 (1H, d, *J* 7.3, 1 x Aromatic CH), 7.80 (1H, d, *J* 7.7, 1 x Aromatic CH); δ_C ($CDCl_3$, 100 MHz) 17.8 (CH_3, $ArCH_3$), 27.8 (CH_2, $ArCH_2$), 97.1 (Cq, C_{spiro}), 116.8 (CH, d, $^2J_{CF}$ 22, 2 x Aromatic CH), 121.9 (d, $^4J_{CF}$ 3.6, 1 x ArCq), 123.5 (CH, 1 x Aromatic CH), 129.4 (CH, 1 x Aromatic CH), 130.2 (1 signal representing 2 x ArCH, d, $^3J_{CF}$ 8), 134.0 (Cq, 1 x Aromatic Cq), 136.7 (Cq, 1 x Aromatic Cq), 137.8 (CH, 1 x Aromatic CH), 150.4 (Cq, 1 x Aromatic Cq), 157.0 (Cq, C=N), 164.6 (Cq, 1 x Aromatic CF, d, $^1J_{CF}$ 255), 192.8 (Cq, C=O); HRMS (ESI+) Exact mass calculated for $C_{17}H_{13}NO_3FS$ $[M+H]^+$, 330.0600. Found: 330.0588.The relative stereochemistry of the cycloadduct **45** was determined by single crystal X-ray diffraction on a crystalline sample of **45** recrystallized from dichloromethane/hexane. Crystals of **45** are orthorhombic, space group Pbca. $\alpha=\beta=\gamma=90°$C, Crystal data for $C_{17}H_{12}NFO_3S$ *Mr* = 329.34, a = 15.237 (3) Å, b = 11.212 (2) Å, c = 17.948 (3) Å, β = 90 (2)°, *V* = 3066.2 (10) $Å^3$, *Z* = 8, D_c = 1.427 g cm^{-3}, F_{000} = 1360, Mo Kα radiation, λ = 0.71073 Å, *T* = 296 K, $2\theta_{max}$ = 67.14°, μ = 2.111 mm^{-1}, 16848 reflections collected, 2637 unique (R_{int} = 0.0398), final GooF = 1.097, R_1 = 0.0448, wR_2 = 0.1302, (2617 obs. data: $I > 2\sigma(I)$); R_1 = 0.0448, wR_2 = 0.1303 (all data). A second fraction isolated from the column contained the 1,4,2-oxathiazole-*S*-oxide Regioisomer **47** (0.026 g, 12%) Yellow crystalline solid; ν_{max}/cm^{-1} (neat) 1724, 1600, 1238, 1080; δ_H (400 MHz, $CDCl_3$); 2.35 (3H, s, CH_3), 3.15 (1H, d, *J* 17.4, A of AB_q, one of CH_2), 3.41 (1H, d, *J* 17.4, B of AB_q, one of CH_2), 7.22 (2H, t, *J* 8.4, 2 x Aromatic CH), 7.47 (2H, t, *J* 8.8, 2 x Aromatic CH), 7.58 (1H, d, *J* 7.2, 2 x Aromatic CH), 7.82 (1H, d, *J* 7.4, 1 x Aromatic CH), 7.94 – 7.97 (2H, m, 2 x Aromatic CH); δ_C ($CDCl_3$, 100 MHz); 17.8 (CH_3, $ArCH_3$), 32.4 (CH_2, $ArCH_2$), 108.2 (Cq, C_{spiro}), 117.0 (CH, 2 x Aromatic CH, d, $^2J_{CF}$ 23.6), 121.5 (Cq, 1 x Aromatic Cq), 122.9, 129.5 (2 x CH, 2 x Aromatic CH), 131.0 (CH, 2 x Aromatic CH, d, $^3J_{CF}$ 8.8), 135.1, 136.4 (Cq, 2 x Aromatic Cq), 137.7 (CH, 1 x Aromatic CH), 146.5 (Cq, 1 x Aromatic Cq), 158.4 (Cq, C=N), 164.8 (Cq, 1 x Aromatic CF, d, $^1J_{CF}$ 256), 189.3 (Cq, C=O); ESI+ $(M+H)^+$ 330 (10%); HRMS (ESI+) Exact mass calculated for $C_{17}H_{13}NO_3FS$ $[M+H]^+$, 330.0600 Found: 330.0594.

4'-(4-(tert-Butyl)phenyl)-4-methylspiro[indene-2,3'-[1,2,5]oxathiazol]-1(*3H*)-one *S*-oxide 48

White crystalline solid (0.041 g, 26%). mp 105 - 106°C; ν_{max}/cm^{-1} (neat) 1721, 1269, 1173; δ_H (400 MHz, $CDCl_3$) 1.28 (9H, s, 3 x CH_3), 2.37 (3H, s, $ArCH_3$), 3.38 (1H, d, *J* 19.2, A of AB_q, one of CH_2), 3.98 (1H, d, *J* 19.2, B of AB_q, one of CH_2), 7.25 (2H, d, *J* 7.9, 2 x Aromatic CH), 7.37 (2H, d, *J* 8.5, 2 x Aromatic CH), 7.48 (1H, t, *J* 7.8, 1 x Aromatic CH), 7.59 (1H, d, *J* 7.3, 1 x Aromatic CH), 7.79 (1H, d, *J* 7.6, 1 x Aromatic CH); δ_C ($CDCl_3$, 100 MHz) 17.9 (CH_3, $ArCH_3$), 28.0 (CH_2, $ArCH_2$), 31.0 (CH_3, 1 signal representing 3 x CH_3), 35.0 [Cq, $Cq(CH_3)_3$], 97.4 (Cq, C_{spiro}), 122.7 (Cq, Aromatic Cq), 123.4 (CH, 1 x Aromatic CH), 126.4, 127.7 (CH, 2 signals representing 4 x Aromatic CH), 129.3 (CH, 1 x Aromatic CH), 134.1 (Cq, 1 x Aromatic Cq), 136.6 (Cq, 1 x Aromatic Cq), 137.6 (CH, 1 x Aromatic CH), 150.5, 155.4 (2 x Cq, 2 x Aromatic Cq), 157.8 (Cq, C=N), 193.0 (Cq, C=O); HRMS (ESI+) Exact mass calculated for $C_{21}H_{22}NO_3S$ $[M+H]^+$, 368.1320. Found: 368.1326.

4-Methyl-4'-(4-nitrophenyl)spiro[indene-2,3'-[1,2,5]oxathiazol]-1(*3H*)-one *S*-oxide 51

White crystalline solid. (0.049 g, 20%). mp 139 – 141°C; ν_{max}/cm^{-1} (neat) 1716, 1521, 1346, 1151; δ_H (400 MHz, $CDCl_3$); 2.32 (3H, s, $ArCH_3$), 3.25 (1H, d, *J* 19.2, A of AB_q, one of CH_2), 4.01 (1H, d, *J* 19.2, B of AB_q, one of CH_2), 7.50 – 7.54 [3H, m overlapping 2H doublet (2 x Aromatic CH) and

1H, m (1 x Aromatic CH)], 7.63 (1H, d, *J* 7.5, 1 x Aromatic CH), 7.82 (1H, d, *J* 7.5, 1 x Aromatic CH), 8.23 (2H, d, *J* 8.8, 2 x Aromatic CH); δ_C ($CDCl_3$, 100 MHz) 17.9 (CH_3, $ArCH_3$), 27.5 (CH_2, $ArCH_2$), 96.5 (Cq, C_{spiro}), 123.7 (CH, 1 x Aromatic CH), 124.5 (CH, 2 x Aromatic CH), 129.0 (CH, 2 x Aromatic CH), 129.7 (CH, 1 x Aromatic CH), 132.0, 133.8, 136.8 (3 x Cq, 3 x Aromatic Cq), 138.1 (CH, 1 x Aromatic CH), 149.5 (Cq, 1 x Aromatic Cq), 150.1 (Cq, 1 x Aromatic Cq), 156.6 (Cq, C=N), 192.3 (Cq, C=O); HRMS (ESI+) Exact mass calculated for $C_{17}H_{13}N_2O_5S$ $[M+H]^+$, 357.0545 Found: 357.0531.

6-Methyl-4'-phenylspiro[indene-2,3'-[1,2,5]oxathiazol]-1(*3H*)-one *S*-oxide 54

Thermodynamic isomer **54** was isolated as a pale yellow solid (0.053g, 34%); Found C, 65.80; H 4.34; N 4.50. $C_{17}H_{13}NO_3S$ requires C, 65.58; H 4.21; N 4.50; m.p. 147-149 °C; ν_{max}/cm^{-1} (neat) 1712, 1276, 1153; δ_H (300 MHz, $CDCl_3$) 2.49 (3H, s, CH_3), 3.42 (1H, d, *J* 19.2, A of AB_q, one of $ArCH_2$), 4.02 (1H, d, *J* 19.2, B of AB_q, one of $ArCH_2$), 7.28 – 7.37 (4H, m, 4 x Aromatic CH), 7.45 – 7.47 (2H, m, 2 x Aromatic CH), 7.59 (2H, dd, *J* 7.7, 1.2, 1 x Aromatic CH), 7.75 (1H, br s, 1 x Aromatic CH); δ_C ($CDCl_3$, 75.5MHz) 21.1 (CH_3, $ArCH_3$), 28.5 (CH_2, $ArCH_2$), 97.7 (Cq, C_{spiro}), 125.7 (Cq, Aromatic Cq), 125.8 (CH, 1 x Aromatic CH), 126.6 (CH, 1 x Aromatic CH), 128.0, 129.3 (2 x CH, 4 x Aromatic CH), 131.6 (CH, 1 x Aromatic CH), 134.4 (Cq, 1 x Aromatic Cq), 138.4 (CH, 1 x Aromatic CH), 139.5 (Cq, 1 x Aromatic Cq), 149.0 (Cq, 1 x Aromatic Cq), 158.0 (Cq, C=N), 192.6 (Cq, C=O); m/z (ESI+) 312 (30%); HRMS (ESI+) Exact mass calculated for $C_{17}H_{14}NO_3S$ $[M+H]^+$, 312.0694 Found: 312.0683. The second fraction to elute was the 1,4,2-oxathiazole-*S*-oxide Regioisomer **56** (0.039 g, 25%) as a white crystalline solid; m.p. 152-154°C (decomp); ν_{max}/cm^{-1} (neat) 1726, 1492, 1282, 1084; δ_H (300 MHz, $CDCl_3$) 2.47 (3H, s, CH_3), 3.26 (1H, d, *J* 17.3, A of AB_q, one of $ArCH_2$), 3.45 (1H, d, *J* 17.3, B of AB_q, one of $ArCH_2$), 7.38 (1H, d, *J* 7.9, 1 x Aromatic CH), 7.48 – 7.59 (4H, m, 4 x Aromatic CH), 7.76 (1H, br s, 1 x Aromatic CH), 7.92 – 7.95 (2H, d, *J* 7.8, 2 x Aromatic CH); δ_C ($CDCl_3$, 75.5 MHz); 21.2 (CH_3, $ArCH_3$), 33.3 (CH_2, $ArCH_2$), 108.5 (Cq, C_{spiro}), 125.2 (Cq, 1 x Aromatic Cq), 125.4, 126.7, 128.8, 129.6, 132.1 (5 signals representing 7 x Aromatic CH), 135.4 (Cq, 1 x Aromatic Cq), 138.3 (CH, 1 x Aromatic CH), 139.7 (Cq, 1 x Aromatic Cq), 144.8 (Cq, 1 x Aromatic Cq), 159.4 (Cq, C=N), 189.0 (Cq, C=O); MS (ESI+) 312 (20%); HRMS (ESI+) Exact mass calculated for $C_{17}H_{14}NO_3S$ $[M+H]^+$, 312.0694. Found: 312.0704.

4'-(4-Fluorophenyl)-6-methylspiro[indene-2,3'-[1,2,5]oxathiazol]-1(*3H*)-one *S*-oxide 57

The thermodynamic isomer **57** (0.032 g, 36%) was isolated as a white crystalline solid; Found C, 61.61; H 3.79; N 4.37. $C_{17}H_{12}NFO_3S$ requires C, 62.00; H 3.67; N 4.25; m.p. 156-158 °C ν_{max}/cm^{-1} (neat) 1711, 1162, 806; δ_H (300 MHz, $CDCl_3$); 2.49 (3H, s, CH_3), 3.40 (1H, d, *J* 19.7, A of AB_q, one of $ArCH_2$), 4.03 (1H, d, *J* 19.7, B of AB_q, one of $ArCH_2$), 7.05 (2H, t, *J* 8.9, 2 x Aromatic CH), 7.28 – 7.34 (2H, m, 2 x Aromatic CH), 7.46 (1H, d, *J* 8.0, 1 x Aromatic CH), 7.61 (1H, d, *J* 7.9, 1 x Aromatic CH), 7.74 (1H, br s, 1 x Aromatic CH); δ_C ($CDCl_3$, 100 MHz); 21.1 (CH_3, $ArCH_3$), 28.4 (CH_2, $ArCH_2$), 97.5 (Cq, C_{spiro}), 116.7 (CH, 1 signal representing 2 x Aromatic CH, d, $^2J_{CF}$ 22.2), 121.9 (Cq, 1 x Aromatic Cq, d, $^4J_{CF}$ 3.3), 125.9 (CH, 1 x Aromatic CH), 126.7 (CH, 1 x Aromatic CH), 130.2 (CH, 2 x ortho Aromatic CH, d, $^3J_{CF}$ 8.7), 134.4, (Cq, 1 x Aromatic Cq), 138.5 (CH, 1 x Aromatic CH), 139.6 (Cq, 1 x Aromatic Cq), 148.9 (Cq, Aromatic Cq), 157.0 (Cq, C=N), 164.6 (Cq, 1 x Aromatic CF, d, $^1J_{CF}$ 254.4), 192.5 (Cq, C=O); MS $(M)^+$ 330 (60%); HRMS (ESI+) Exact mass calculated for $C_{17}H_{13}FNO_3S$ $[M+H]^+$, 330.0600 Found: 330.0600. The second fraction to elute isolated contained the kinetic 1,2,5-oxathiazole-*S*-oxide **58** (0.004 g, 5%), δ_H (400 MHz, $CDCl_3$) 2.49 (3H, s, CH_3), 3.53 (1H, d, *J* 18.5, A of AB_q, one of $ArCH_2$), 3.77 (1H, d, *J* 18.5, B of AB_q, one of $ArCH_2$), 7.03 (2H, t, *J* 8.9, 2 x Aromatic CH), 7.45– 7.51 (3H, m, 3 x Aromatic CH), 7.58 – 7.63 (1H, m, 1 x Aromatic CH), 7.75 (1H, br s, 1 x Aromatic CH); $(M+H)^+$ 330 (25%), HRMS (ESI+) Exact mass calculated for $C_{17}H_{13}NO_3FS$ $[M+H]^+$, 330.0600. Found: 330.0605. The third, most polar fraction to elute contained the 1,4,2-oxathiazole-*S*-oxide regioisomer **59** (0.008 g, 10%) as a colorless oil; ν_{max}/cm^{-1} (neat) 1722, 1282, 1157, 1083; δ_H (600 MHz, $CDCl_3$) 2.47 (3H, s, CH_3), 3.26 (1H, d, *J* 17.3, A of AB_q, one of $ArCH_2$), 3.45 (1H, d, *J* 17.3, B of AB_q, one of $ArCH_2$), 7.22 (2H, t, *J* 8.4, 2 x Aromatic CH), 7.39 (1H, d, *J* 7.7, 1 x Aromatic CH), 7.56 – 7.60 (1H, d, *J* 8.3, 1 x Aromatic CH), 7.76 (1H, s, 1 x Aromatic CH), 7.92 – 7.97 (2H, m, 2 x Aromatic CH); δ_C ($CDCl_3$, 125 MHz) 21.2 (CH_3, $ArCH_3$), 33.3 (CH_2, $ArCH_2$), 108.7 (Cq, C_{spiro}), 117.0 (CH, 2 x ArCH, d, $^2J_{CF}$ 22.6), 121.4 (Cq, d, $^4J_{CF}$ 3.3, 1 x Aromatic Cq), 125.4, 126.7 (CH, 2 x Aromatic CH), 131.0 (CH, 2 x Aromatic CH, d, $^3J_{CF}$ 9.4), 135.3 (Cq, 1 x Aromatic Cq), 138.4 (CH, 1 x Aromatic CH), 139.8, 144.7 (2 x Cq, 2 x Aromatic Cq), 158.4 (Cq, C=N), 164.9 (Cq, 1 x Aromatic CF, d, $^1J_{CF}$ 254), 188.9 (Cq, C=O); MS $(M)^+$ 329 (100%); HRMS (ESI+) Exact mass calculated for $C_{17}H_{12}FNO_3SNa$ $[M+Na]^+$, 352.0420 Found: 352.0425.

6-Methyl-4'-(4-nitrophenyl)spiro[indene-2,3'-[1,2,5]oxathiazol]-1(*3H*)-one *S*-oxide 62

Thermodynamic isomer **62** was isolated as a white crystalline solid (0.100 g, 45%). Found C, 56.95; H 3.49; N 7.75. $C_{17}H_{12}N_2O_5S$ requires C, 57.30; H 3.39 ; N 7.86; m.p. 128 – 130°C; ν_{max}/cm^{-1} (neat) 1707, 1523 1345, 1154; δ_H (300 MHz, $CDCl_3$) 2.50 (3H, s, CH_3), 3.35 (1H, d, *J* 19.4, A of AB_q, one of $ArCH_2$), 4.07 (1H, d, *J* 19.4, B of AB_q, one of $ArCH_2$), 7.47 – 7.53 [3H, 2 overlapping signals; (1H, d, *J* 8.5) and (2H, d, *J* 9.1, 2 x Aromatic CH)], 7.63 (1H, d, *J* 8.1, 1 x Aromatic CH), 7.77 (1H, br s, 1 x Aromatic CH), 8.22 (2H, d, *J* 9.0, 2 x Aromatic CH); δ_C ($CDCl_3$, 75 MHz) 21.2 (CH_3, $ArCH_3$), 28.1 (CH_2, $ArCH_2$), 96.8 (Cq, C_{spiro}), 124.5 (CH, 2 x Aromatic CH), 126.1 (CH, 1 x Aromatic CH), 126.8 (CH, 1 x Aromatic CH), 129.0 (CH, 2 x Aromatic CH), 132.0, 134.2 (Cq, 2 x Aromatic Cq), 138.8 (CH, 1 x Aromatic CH), 140.0, 148.6, 149.5 (Cq, 3 x Aromatic Cq), 156.0 (Cq, C=N) 192.0 (Cq, C=O); HRMS (ESI+) Exact mass calculated for $C_{17}H_{13}N_2O_5S$ $[M+H]^+$, 357.0545. Found: 357.0549. A second fraction contained the kinetic 1,2,5-oxathiazole-*S*-oxide diastereomer **63** (0.027 g, 11%); ν_{max}/cm^{-1} (neat) 1714, 1522, 1347; δ_H (300 MHz, $CDCl_3$) 2.51 (3H, s, CH_3), 3.54 (1H, d, *J* 18.0, A of AB_q, one of $ArCH_2$), 3.82 (1H, d, *J* 18.0, B of AB_q, one of $ArCH_2$), 7.49 – 7.54 (1H, m, 1 x Aromatic CH), 7.61 – 7.72 [3H, 2 overlapping signals (1H, m, 1 x Aromatic CH) and (2H, d, *J* 9.0, 2 x Aromatic CH)], 7.75 (1H, br s, 1 x Aromatic CH), 8.20 (2H, d, *J* 9.0, 2 x Aromatic CH); δ_C ($CDCl_3$, 75 MHz) 21.2 (CH_3, $ArCH_3$), 31.3 (CH_2, $ArCH_2$), 92.8 (Cq, C_{spiro}), 124.21 (Cq, 1 x Aromatic Cq), 124.3 (CH, 2 x Aromatic CH), 125.6 (CH, 1 x Aromatic CH), 126.8 (CH, 1 x Aromatic CH), 129.1 (CH, 2 x Aromatic CH), 131.7 (Cq, 1 x Aromatic Cq), 136.5 (Cq, 1 x Aromatic Cq), 138.5 (CH, 1 x Aromatic CH), 140.3, 146.2 (Cq, 2 x Aromatic Cq), 157.6 (Cq, C=N), 190.3 (Cq, C=O); HRMS (ESI+) Exact mass calculated for $C_{17}H_{13}N_2O_3S$ $[M+H]^+$, 357.0545. Found: 357.0540.

4'-(4-(tert-Butyl)phenyl)-6-methylspiro[indene-2,3'-[1,2,5]oxathiazol]-1(*3H*)-one *S*-oxide 60

60 was isolated as a yellow oil (0.030 g, 15%). ν_{max}/cm^{-1} (neat) 2963, 1714, 1156, 814; δ_H (300 MHz, $CDCl_3$); 1.27 (9H, s, 3 x CH_3), 2.49 (3H, s, $ArCH_3$), 3.47 (1H, d, *J* 19.0, A of AB_q, one of $ArCH_2$), 4.03 (1H, d, *J* 19.0, B of AB_q, one of $ArCH_2$), 7.24 (2H, d, *J* 8.5, 2 x Aromatic CH), 7.36 (2H, d, *J* 8.6, 2 x Aromatic CH), 7.45 (1H, d, *J* 7.9, 1 x Aromatic CH), 7.59 (1H, d, *J* 7.8, 1 x Aromatic CH), 7.74 (1H, br s, 1 x Aromatic CH); δ_C ($CDCl_3$, 75.5 MHz) 21.1 (CH_3, $ArCH_3$) 28.7 (CH_2, $ArCH_2$), 31.0 (CH_3, 1 signal representing 3 x CH_3), 35.0 [Cq, $C(CH_3)_3$], 97.8 (Cq, C_{spiro}), 122.7 (Cq, Aromatic Cq), 125.8 (CH, 1 x Aromatic CH), 126.4 (CH, 2 x Aromatic CH), 126.6 (CH, 1 x Aromatic CH), 127.8 (CH, 2 x Aromatic CH), 134.6 (Cq, 1 x Aromatic Cq), 138.3 (CH, 1 x Aromatic CH), 139.4, 149.1, 155.3 (3 x Cq, 3 x Aromatic Cq), 157.8 (Cq, C=N), 192.7 (Cq, C=O); (M+H) 368 (60%); HRMS (ESI+) Exact mass calculated for $C_{21}H_{22}NO_3S$ $[M+H]^+$, 368.1320. Found: 368.1306.

4'-(2,5-Difluorophenyl)-6-methylspiro[indene-2,3'-[1,2,5]oxathiazol]-1(*3H*)-one *S*-oxide 65

The thermodynamic isomer **65** was isolated as the major component of one fraction as a brown oil (~90% pure, 0.026 g, 16%). ν_{max}/cm^{-1} (neat) 1720, 1490, 1429, 1163; δ_H (300 MHz, $CDCl_3$) 2.46 (3H, s, $ArCH_3$), 3.31 (1H, d, *J* 18.8, A of AB_q, one of $ArCH_2$), 3.94 (1H, d, *J* 18.6, B of AB_q, one of $ArCH_2$), 7.01 (1H, t of d, *J* 9.4, 4.3, 1 x Aromatic CH), 7.13 – 7.22 (1H, m, 1 x Aromatic CH), 7.39 (1H, d, *J* 7.9, 1 x Aromatic CH), 7.46 – 7.51 (1H, m, 1 x Aromatic CH), 7.55 (1H, d, *J* 7.5, 1 x Aromatic CH), 7.71 (1H, br s, 1 x Aromatic CH). Characteristic signals of **65** identified in the ^{13}C NMR spectrum include; δ_C ($CDCl_3$, 75.5 MHz); 21.1 (CH_3, $ArCH_3$) 27.9 (CH_2, $ArCH_2$), 97.5 (Cq, C_{spiro}), 117.5 – 118.3 (2 overlapping dd corresponding to 2 x Aromatic CH, including 1d $^3J_{CF}$ 8.8, 1d $^4J_{CF}$ 3.3), 120.5 (CH, 1 x Aromatic CH, dd, $^2J_{CF}$ 25, $^3J_{CF}$ 9.3), 125.8 (CH, 1 x Aromatic CH), 126.3 (CH, 1 x Aromatic CH), 137.8 (CH, 1 x Aromatic CH), 148.5 (Cq, C=N), 156.2 (Cq, 1 x Aromatic CF, d, $^1J_{CF}$ 260), 158.6 (Cq, 1 x Aromatic CF, d, $^1J_{CF}$ 246), 191.1 (Cq, C=O); MS $(M)^+$ 347 (15%), HRMS (ESI+) Exact mass calculated for $C_{17}H_{12}NO_3F_2S$ $[M+H]^+$, 348.0506. Found: 348.0515

References

(1) Y. Cui and P. E. Floreancig, *Org. Lett.*, 2012, **14**, 1720.
(2) M. R. Prinsep, In *Stud. Nat. Prod. Chem.*; Atta-ur, R., Ed.; Elsevier: 2003; **Vol. 28**, Part I, p 617.
(3) K. Jayakanthan, S. Mohan and B. M. Pinto, *J. Am. Chem. Soc.*, 2009, **131**, 5621.
(4) A. E. Aliev, K. Karu, R. E. Mitchell and M. J. Porter, *Org. Biomol. Chem.*, 2016, **14**, 238.
(5) B. C. Lemercier and J. G. Pierce, *Org. Lett.*, 2015, **17**, 4542.
(6) G. Mlostoń, M. K. Kowalski, E. Obijalska and H. Heimgartner, *J. Fluorine Chem.*, 2017, **199**, 92.
(7) S. Hornbuckle, P. Livant and T. Webb, *J. Org. Chem.*, 1995, **60**, 4153.
(8) A. Tsolomitis and C. Sandris, *J. Heterocycl. Chem.*, 1984, **21**, 1679.
(9) H.-Z. Zhang, S. Kasibhatla, J. Kuemmerle, W. Kemnitzer, K. Ollis-Mason, L. Qiu, C. Crogan-Grundy, B. Tseng, J. Drewe and S. X. Cai, *J. Med. Chem.*, 2005, **48**, 5215.
(10) B. F. Bonini, G. Maccagnani, G. Mazzanti, L.Thijs, H. P. M. M. Ambrosius and B. Zwanenburg, *J. Chem. Soc., Perkin Trans. 1,* 1977, 1468.
(11) B. F. Bonini, G. Maccagnani, G. Mazzanti, P. Pedrini, B. H. M. Lammerink and B. Zwanenburg, *J. Chem. Soc., Perkin Trans. 1,* 1983, 2097.
(12) B. Zwanenburg, *Recl. Trav. Chim. Pays-Bas,* 1982, **101**, 1.
(13) Y. W. Lim, R. J. Hewitt and B. A. Burkett, *Eur. J. Org. Chem.,* 2015, 4840.
(14) B. A. Burkett, P. Fu, R. J. Hewitt, S. L. Ng and J. D. W. Toh, *Eur. J. Org. Chem.,* 2014, **5**, 1053.
(15) O. C. M. O'Sullivan, S. G. Collins, A. R. Maguire, M. Böhm and W. Sander, *Eur. J. Org. Chem.,* 2006, 2918.
(16) O. O'Sullivan, S. Collins and A. Maguire, *Synlett,* 2008, 659.
(17) O. C. M. O'Sullivan, S. G. Collins, A. R. Maguire and G. Bucher, *Eur. J. Org. Chem.,* 2014, 2297.
(18) S. G. Collins, O. C. M. O'Sullivan, P. G. Kelleher and A. R. Maguire, *Org. Biomol. Chem.,* 2013, **11**, 1706.
(19) P. G. McCaw, B. J. Deadman, A. R. Maguire and S. G. Collins, *J. Flow Chem.,* 2016, **6**, 226.
(20) B. J. Deadman, R. M. O'Mahony, D. Lynch, D. C. Crowley, S. G. Collins and A. R. Maguire, *Org. Biomol. Chem.,* 2016, **14**, 3423.
(21) A. R. Maguire, S. G. Collins and A. Ford, *Arkivoc,* 2003, **7**, 96.
(22) B. J. Deadman, S. G. Collins and A. R. Maguire, *Chem. Eur. J.*, 2015, **21**, 2298.
(23) I. M. Mándity, S. B. Ötvös and F. Fülöp, *Chem. Open,* 2015, **4**, 212.
(24) A. Adamo, R. L. Beingessner, M. Behnam, J. Chen, T. F. Jamison, K. F. Jensen, J.-C. M. Monbaliu, A. S. Myerson, E. M. Revalor, D. R. Snead, T. Stelzer, N. Weeranoppanant, S. Y. Wong and P. Zhang, *Science*, 2016, **352**, 61.
(25) T. Tsubogo, H. Oyamada and S. Kobayashi, *Nature*, 2015, **520**, 329.
(26) R. Porta, M. Benaglia and A. Puglisi, *Org. Pro. Res. Dev.*, 2016, **20**, 2.
(27) M. Trojanowicz, *Talanta*, 2016, **146**, 621.
(28) F. Lévesque, N. J. Rogus, G. Spencer, P. Grigorov, J. P. McMullen, D. A. Thaisrivongs, I. W. Davies and J. R. Naber, *Org. Pro. Res. Dev.*, 2018, **22**, 1015.
(29) K. P. Cole, J. M. Groh, M. D. Johnson, C. L. Burcham, B. M. Campbell, W. D. Diseroad, M. R. Heller, J. R. Howell, N. J. Kallman, T. M. Koenig, S. A. May, R. D. Miller, D. Mitchell, D. P. Myers, S. S. Myers, J. L. Phillips, C. S. Polster, T. D. White, J. Cashman, D. Hurley, R. Moylan, P. Sheehan, R. D. Spencer, K. Desmond, P. Desmond and O. Gowran, *Science*, 2017, **356**, 1144.
(30) M. C. Damião, R. Galaverna, A. P. Kozikowski, J. Eubanks and J. C. Pastre, *React. Chem. Eng.*, 2017, **2**, 896.
(31) S. G. Newman and K. F. Jensen, *Green Chem.*, 2013, **15**, 1456.
(32) I. R. Baxendale, L. Brocken and C. J. Mallia, *In Green Process. Synth.*, 2013; **Vol. 2**, p 211.
(33) G. A. Price, M. Debasis and M. G. Organ, *J. Flow Chem.*, 2017, **7**, 82.
(34) K. Poscharny, D. C. Fabry, S. Heddrich, E. Sugiono, M. A. Liauw and M. Rueping, *Tetrahedron*, 2018, **74**, 3171.
(35) D. E. Fitzpatrick, C. Battilocchio and S. V. Ley, *Org. Pro. Res. Dev.*, 2016, **20**, 386.

(36) R. Labes, C. Battilocchio, C. Mateos, G. R. Cumming, O. de Frutos, J. A. Rincón, K. Binder and S. V. Ley, *Org. Pro. Res. Dev.* 2017, **21**, 1419.
(37) M. J. Pedersen, T. Skovby, M. J. Mealy, K. Dam-Johansen and S. Kiil, *Org. Pro. Res. Dev.*, 2018, **22**, 228.
(38) L. Huck, A. de la Hoz, A. Díaz-Ortiz and J. Alcázar, *Org. Lett.*, 2017, **19**, 3747.
(39) H. Seo, M. H. Katcher and T. F. Jamison, *Nat. Chem.*, 2017, **9**, 453.
(40) B. L. Ramsey, R. M. Pearson, L. R. Beck and G. M. Miyake, *Macromolecules*, 2017, **50**, 2668.
(41) Y. Su, N. J. W. Straathof, V. Hessel and T. Noël, *Chem. Eur. J.,* 2014, **20**, 10562.
(42) B. F. Bonini, G. Maccagnani, A. Wagenaar, L. Thijs and B. Zwanenburg, *J. Chem. Soc., Perkin Trans. 1,* 1972, 2490.
(43) A. Elsäßer, W. G. Sundermeyer, *Chem. Ber.,* 1985, **118**, 4553.
(44) G. Mlostoń, A. Linden and H. Heimgartner, *Helv. Chim. Acta,* 1996, **79**, 31.
(45) M. Teci, M. Tilley, M. A. McGuire and M. G. Organ, *Org. Pro. Res. Dev.*, 2016, **20**, 1967.
(46) M. Grafton, A. C. Mansfield and M. J. Fray, *Tetrahedron Lett.*, 2010, **51**, 1026.
(47) S. B. Ötvös, I. M. Mándity, L. Kiss and F. Fülöp, *Chemistry–An Asian Journal,* 2013, **8**, 800.
(48) P. G. McCaw, N. M. Buckley, K. S. Eccles, S. E. Lawrence, A. R. Maguire and S. G. Collins, *J. Org. Chem.,* 2017, **82**, 3666.
(49) M. Kissane, S. E. Lawrence and A. R. Maguire, *Tetrahedron,* 2010, **66**, 4564.
(50) P. G. McCaw, N. M. Buckley, S. G. Collins and A. R. Maguire, *Eur. J. Org. Chem.,* 2016, 1630.
(51) B. Zwanenburg, *J. Sulfur Chem.* 2013, **34**, 142.
(52) B. F. Bonini, G. Maccagnani, G. Mazzanti, L. Thijs, G. E. Veenstra and B. Zwanenburg, *J. Chem. Soc., Perkin Trans. 1,* 1978, 1218.
(53) J. Hejmanowska, M. Jasiński, G. Mlostoń and Ł. Albrecht, *Eur. J. Org. Chem.,* 2017, 950.
(54) R. Huisgen, G. Mloston and K. Polborn, *J. Org. Chem.,* 1996, **61**, 6570.
(55) C. Henry, D. Bolien, B. Ibanescu, S. Bloodworth, D. C. Harrowven, X. Zhang, A. Craven, H. F. Sneddon and R. J. Whitby, *Eur. J. Org. Chem.,* 2015, 1491.
(56) N. Lamborelle, J. F. Simon, A. Luxen and J.-C. M. Monbaliu, *Org. & Bio. Chem.,* 2015, **13**, 11602.
(57) A. G. O'Brien, F. Levesque and P. H. Seeberger, *Chem. Commun.,* 2011, **47**, 2688.
(58) M. Brasholz, S. Saubern and G. P. Savage, *Aust. J. Chem.,* 2011, **64**, 1397.
(59) M. Schwab and W. Sundermeyer, *Chem. Ber.,* 1988, **121**, 75.
(60) J. C. Dyer, S. A. Evans, *J. Org. Chem.,* 1980, **45**, 5350.
(61) J. B. M. Rewinkel and B. Zwanenburg, *Recl. Trav. Chim. Pays-Bas,* 1990, **109**, 190.
(62) B. E. Gryder, W. Guerrant, C. H. Chen and A. K. Oyelere, *Med. Chem. Commun.,* 2011, **2**, 1083.
(63) L. Somsák, V. Nagy, S. Vidal, K. Czifrák, E. Berzsényi and J.-P. Praly, *Biorg. Med. Chem. Lett.,* 2008, **18**, 5680.
(64) G. Lin, D. Li, L. P. S. de Carvalho, H. Deng, H. Tao, G. Vogt, K. Wu, J. Schneider, T. Chidawanyika, J. D. Warren, H. Li and C. Nathan, *Nature,* 2009, **461**, 621.